MESOZOIC MAGMATISM IN MONTANA

Kaleb C. Scarberry,[1] Petr V. Yakovlev,[1] and Theresa M. Schwartz[2]

[1]*Montana Bureau of Mines and Geology, Butte, Montana*

[2]*U.S. Geological Survey, Denver, Colorado*

ABSTRACT

From crystalline batholiths with footprints larger than 4,500 km^2 to beds of micron-sized ash particles, a record of Mesozoic magmatism is found throughout Montana. Mesozoic igneous rocks are an important natural resource in the State because of their association with precious metal ores and industrial mineral deposits. Mesozoic magmatism in Montana is a tale of volcanic arc eruptions, pluton emplacement, crustal magma differentiation, melting, and assimilation. Explosive caldera-forming eruptions, magmatic hydrothermal and metamorphic mineralization, tectonic uplift, fluvial erosion, and redeposition of igneous rocks and mineral resources are all chronicled by Mesozoic igneous rocks. This article offers a summary of the types, locations, extents, and ages of Mesozoic igneous rocks in Montana. There follows a discussion of the generation and emplacement of magmas and intrusive rocks, their geometries, and the style and timing of magmatism. The article ends with a summary of what remains unknown and offers suggestions for future research.

INTRODUCTION

Montana prospectors have long recognized the association among lode gold systems, stream placers, and crystalline igneous rocks. Gold strikes at Grasshopper Creek (1862), Alder Gulch (1863), and Last Chance Gulch (1864) drew swarms of prospectors to southwestern Montana (summary in Albright, 2004) and sparked the charge toward scientific inquiries into the nature of Mesozoic igneous systems and their mineral deposits. Lindgren (1886) first described granite at Mullan Pass, about 10 mi (16 km) northwest of Helena (fig. 1), and laid the foundation for subsequent research.

North American Cordilleran arc magmatism was underway by the Jurassic in southern California, prior to breakup of the supercontinent Pangea (Coney, 1972; Dickinson and others, 1988; Miller and Snoke, 2009; Sauer and others, 2017), and reached Montana during the Late Cretaceous. Pyroclastic ash-fall deposits from silicic eruptions settled in the Western Interior of the United States (fig. 2), in shallow marine and continental settings and inland of the Cordilleran arc that developed along the western margin of the continent. In Montana, arc-related deposits include ashes derived from the Jurassic–Early Cretaceous arc that was located along the continental margin (the Sierra Nevada Batholith) as well as ashes derived from the Late Cretaceous arc located in the continental interior (the Idaho and Boulder Batholiths; Christiansen and others, 1994).

Mesozoic igneous rocks dominantly formed in Montana between about 120 Ma and 66 Ma (fig. 3) and include batholiths, plutons, volcanic fields, epiclastic volcanic sedimentary aprons, and pyroclastic ash beds (bentonite). Magmatism continued into the Cenozoic (fig. 3) as the Cordilleran arc collapsed and regional stresses transitioned to an extensional regime (Mosolf and others, this volume). Most workers agree that (1) batholiths and plutons formed in an evolving thrust wedge during Late Cretaceous contractional deformation (Tilling and others, 1968; Hamilton, 1988; Lageson and others, 2001); (2) batholiths, plutons, and related volcanic rocks are a record of Cordilleran arc magmatism (Rutland and others, 1989; Saleeby and others, 1992; Gaschnig and others, 2011);

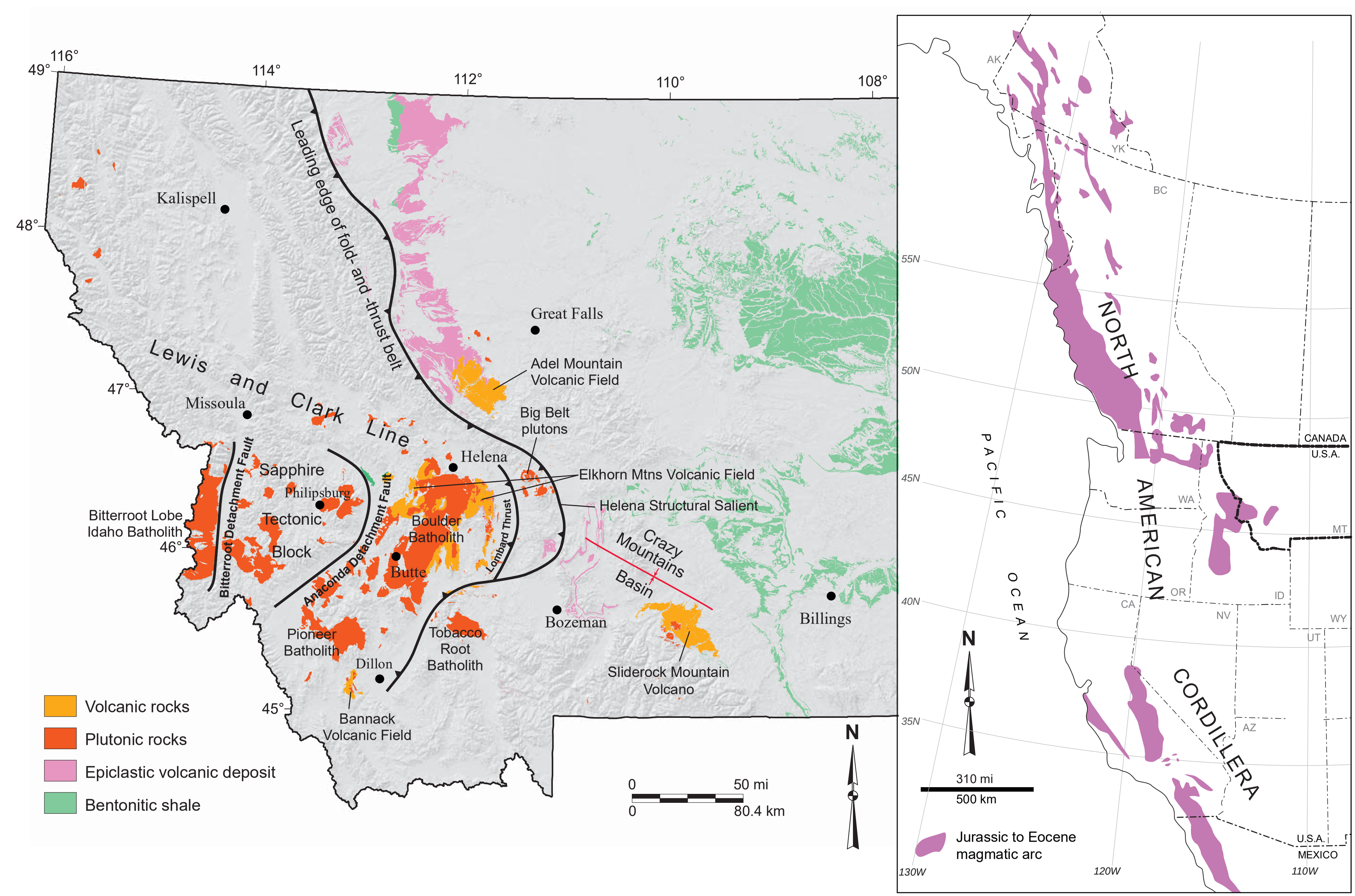

Figure 1. Distribution of Mesozoic magmatic arc and related rocks in Montana. Inset panel modified from Sauer and others, 2017. Distribution of the Jurassic to Eocene arc in North America after Burchfiel and others (1992).

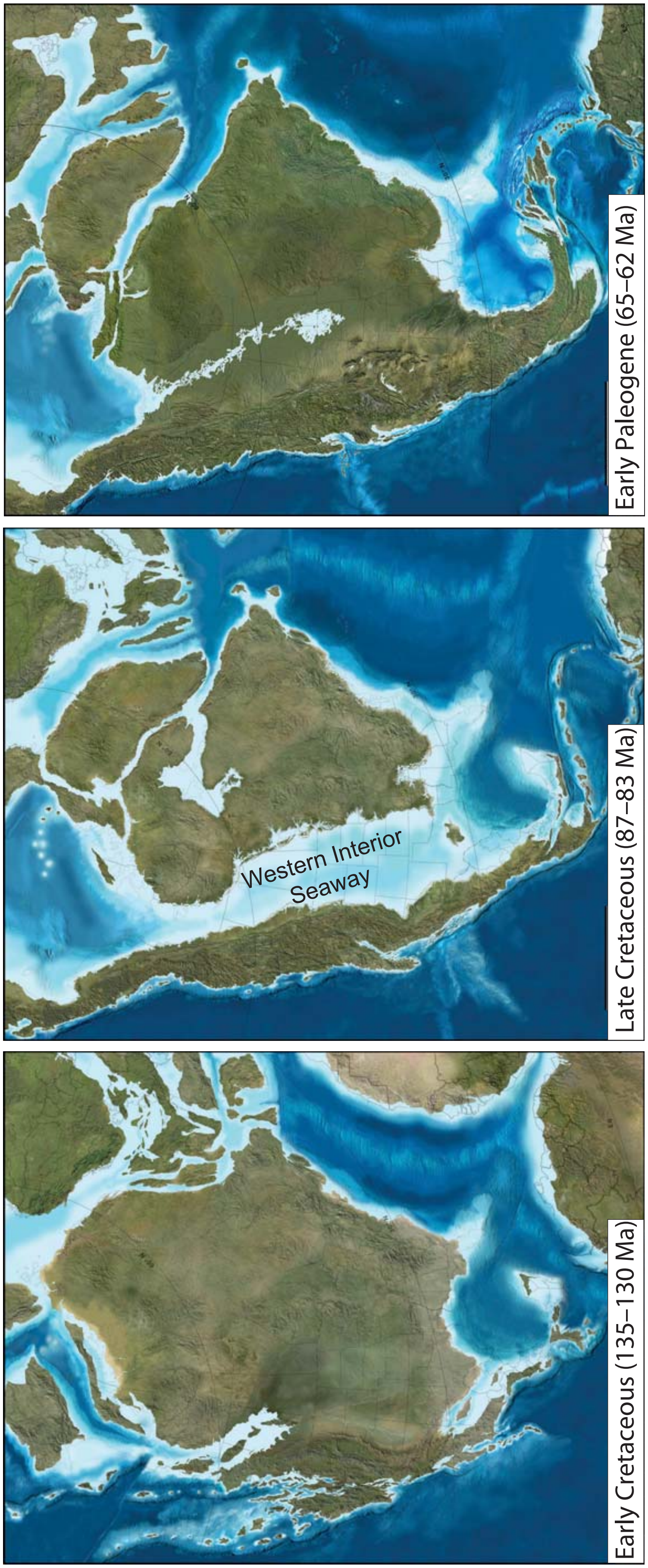

Figure 2. Early Cretaceous through early Paleogene paleogeographic maps. From Blakey, https://deeptimemaps.com, with permission (Blakey, 2016)..

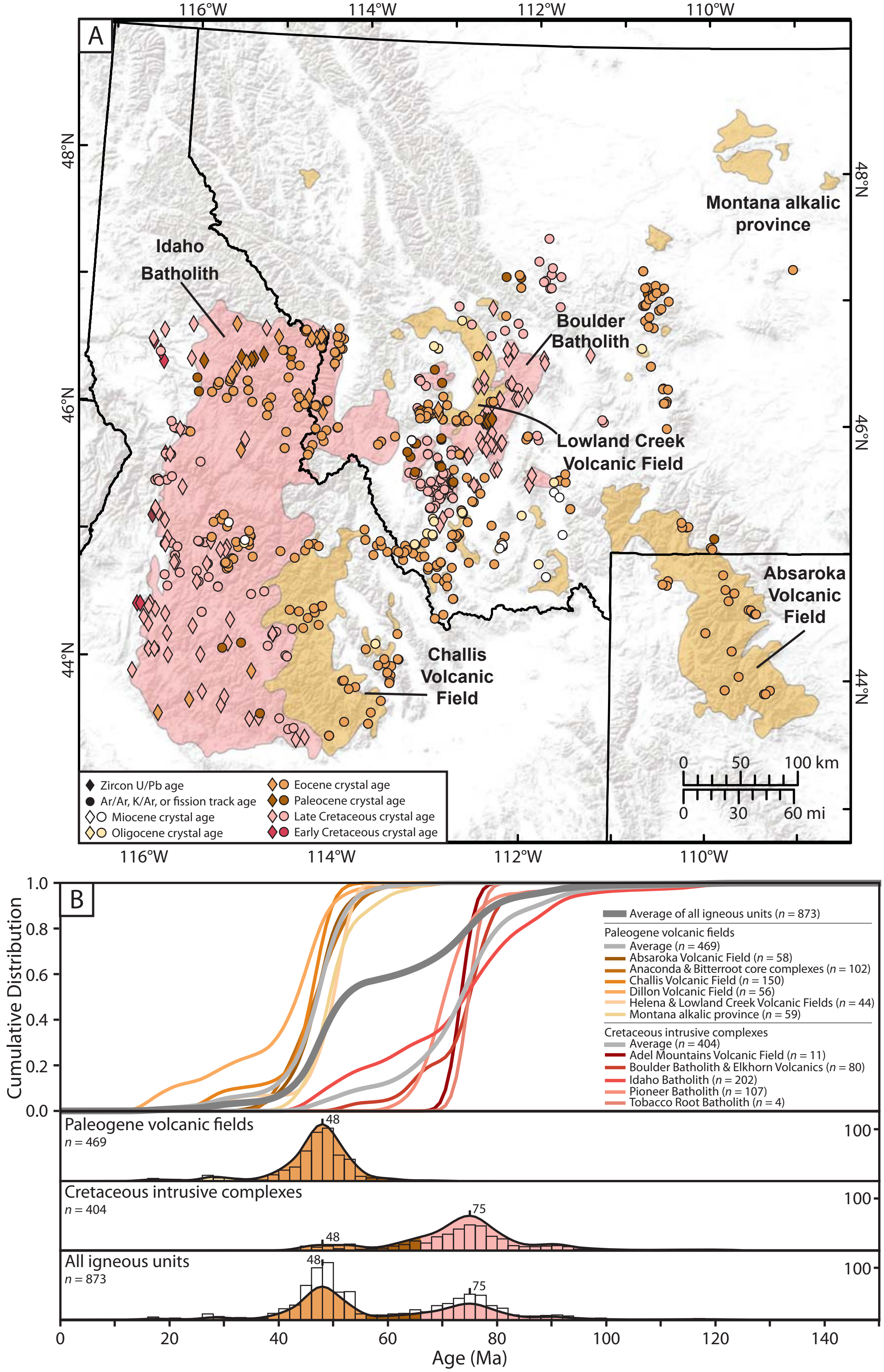

Figure 3. Age constraints on Cretaceous and Paleogene igneous complexes in western Montana and adjacent areas. (A) Hillshade map showing the spatial distribution of Cretaceous intrusive (pink) and Paleogene volcanic (orange) complexes and the locations of geochronologic age constraints from U/Pb, $^{40}Ar/^{39}Ar$, K/Ar, and fission track analyses (compilation from Schwartz and others, 2019b). Basemap data from Esri, USGS, and NOAA. (B) Cumulative probability curves and kernel density estimates (bandwidth = 2; histogram bins = 2 Ma) for Cretaceous intrusive and Paleogene volcanic complexes based on compiled U/Pb, $^{40}Ar/^{39}Ar$, K/Ar, and fission track ages.

(3) Paleocene uplift followed by Paleocene–Eocene fluvial incision (e.g., Houston and Dilles, 2013; Schwartz and others, 2019a) removed cogenetic volcanic deposits from atop many batholiths and plutons; and (4) collectively, these processes contributed to the production and distribution of lode gold systems and stream placer deposits throughout southwestern Montana (Lyden, 1948; Foster and Childs, 1993; see contributions to this special publication, volume 2, by Reed and Dilles, 2020, and Gammons and others, 2020).

BATHOLITHS AND PLUTONS

Mesozoic intrusions in Montana occur primarily within and adjacent to the Helena structural salient (fig. 1) and include large batholiths and smaller plutons (fig. 4). The Idaho, Boulder, and Pioneer Batholiths are the major intrusive centers in Montana. Smaller batholiths, such as the Philipsburg, Mount Powell, and Tobacco Root Batholiths, are satellite masses to the major intrusive centers. Paleogene volcanic fields that postdate regional arc-related magmatism include the Absaroka, Challis, Dillon, and Lowland Creek volcanic fields, and lie adjacent to and partly overprint the Mesozoic intrusive centers (fig. 3).

Figure 3 shows the spatial distribution of available emplacement and eruption ages of Late Cretaceous and Paleogene igneous provinces in western Montana and adjacent Idaho (modified from Schwartz and others, 2019b). In general, igneous activity was continuous between latest Cretaceous and Paleogene time, with episodes of higher apparent magmatic flux occurring between ca. 85–70 Ma and ca. 55–45 Ma (fig. 3; Gaschnig and others, 2011; this study). The ca. 85–70 Ma pulse of igneous activity corresponds to emplacement of the Idaho, Boulder, and associated batholiths/plutons in western Montana and eastern Idaho in response to Sevier–Laramide plate subduction (ca. 110–87 Ma), subsequent crustal thickening, and attendant crustal melting (ca. 83–54 Ma; Gaschnig and others, 2011). Contraction-related magmatism was closely followed by extension-related magmatism (ca. 54–43 Ma), associated with extensional collapse of overthickened crust (Gaschnig and others, 2011). Given the transitional nature of magmatism from contraction- to extension-related at the Cretaceous–Paleogene boundary, some Late Cretaceous magmatic complexes host plutons with Paleogene crystallization ages (e.g., the Idaho Batholith; fig. 3). Such plutons are included in this summary because they formed by geologic processes identical to their Late Cretaceous precursors.

Idaho Batholith and Sapphire Block Plutons

The Late Cretaceous–Paleogene Idaho Batholith contains two lobes, the northern Bitterroot lobe and the larger southern Atlanta lobe, which is not exposed in Montana. The batholith intruded Proterozoic basement rocks (Hyndman, 1983). About 200 km^2 of the Bitterroot lobe, less than 10% of the total 25,000 km^2 footprint of the Idaho Batholith, extends into Montana (fig. 1). Both lobes are composed of texturally similar biotite granodiorite, yet the Bitterroot lobe is conspicuously younger (66 to 53 Ma) than the Atlanta lobe (83 to 67 Ma; Foster and Fanning, 1997; Gaschnig and others, 2011). The Atlanta lobe of the batholith contains 98–87 Ma hornblende-bearing roof pendants and stocks along its southeast margin (Gaschnig and others, 2011). East of the Bitterroot lobe, several outlier granitic plutons similar in composition to the Idaho Batholith are exposed over a 700 km^2 arcuate area called the Sapphire block (fig. 1; Hyndman and others, 1975).

Boulder Batholith and Satellite Intrusions

The Boulder Batholith extends from Butte to Helena (fig. 1) and consists of about 15 plutons exposed over 4,500 km^2. The roof of the batholith crystallized beneath a cover of volcanic rocks of similar age and composition over a period of about 8 Ma (Tilling and others, 1968; Olson and others, 2017). The batholith is largely zoned in terms of age and composition (Tilling and others, 1968; Klepper and others, 1971a; du Bray and others, 2012). Granodiorite to gabbro plutons along the north, east, and southern margins of the batholith crystallized between about 81 and 76 Ma, whereas the principal body, the Butte pluton (fig. 4), formed between about 76 and 76.5 Ma (du Bray and others, 2012; Olson and others, 2017). Two world-class porphyry Cu-Mo deposits overprinted by a vast system of zoned polymetallic Cu-Zn-Pb-Mn-Ag lode veins (Rusk and others, 2008; summaries in Czehura, 2006; Houston and Dilles, 2013) formed during emplacement of the Boulder Batholith–Elkhorn Mountains Volcanics magma system (Lund and others, 2002, 2018).

Pioneer Batholith

The Pioneer Batholith, located northwest of Dillon (fig. 1), is a composite of at least 15 plutons that intruded Proterozoic–Mesozoic rocks over an area

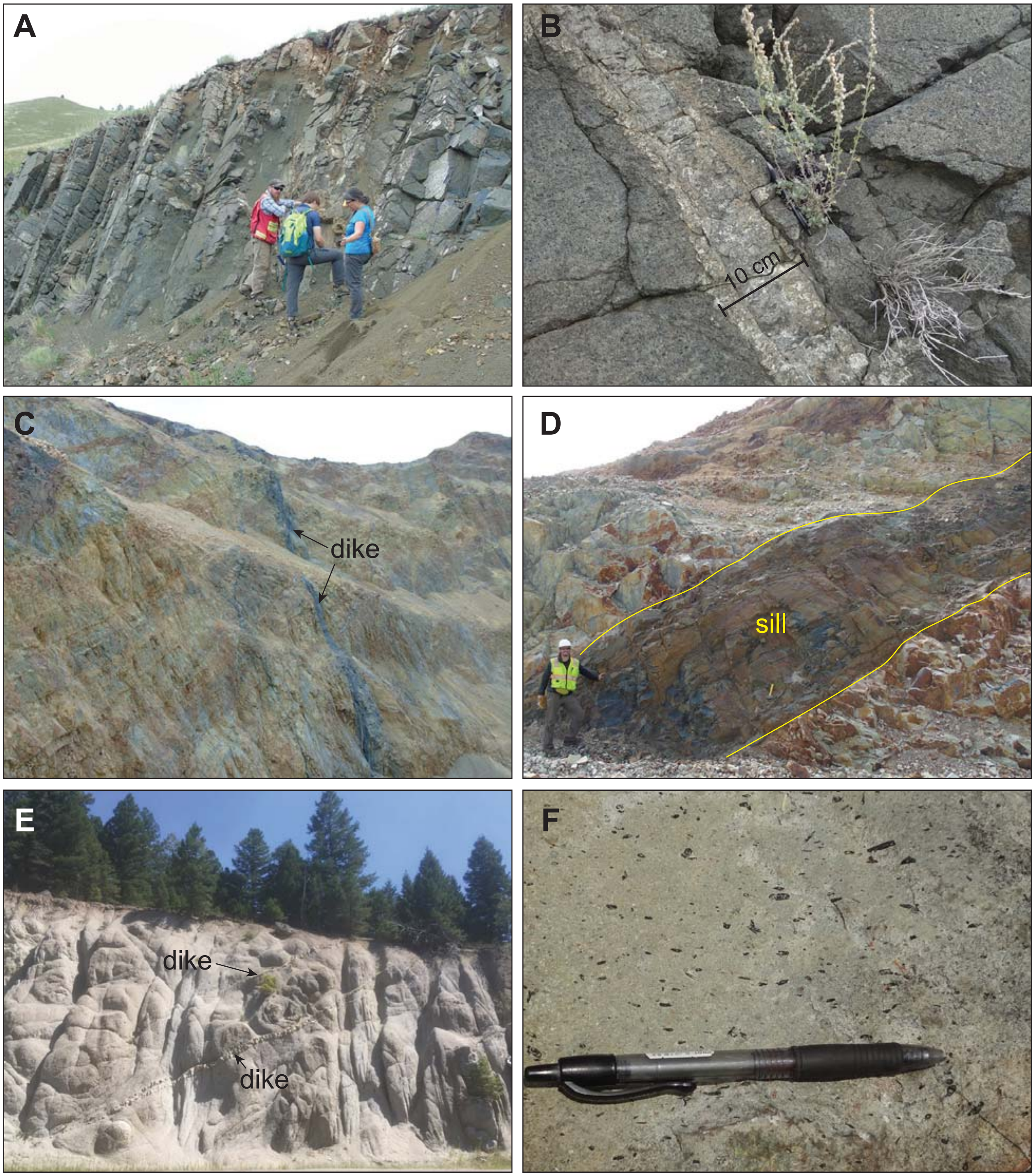

Figure 4. Mesozoic intrusive rocks. (A) Gabbro laccolith exposed south of Big Chief Park on Bull Mountain, Jefferson County. (B) Lamprophyre dike (10 cm wide) cuts gabbro south of Big Chief Park on Bull Mountain. (C) Lamprophyre dike cuts Mesoproterozoic Belt Supergroup rocks in the main pit wall of the Golden Sunlight Mine, Jefferson County. (D) Gabbro sill cuts Mesoproterozoic Belt Supergroup rocks at the Golden Sunlight Mine. (E) Butte Granite exposed near the northern entrance to Thompson Park, south of Butte, Silver Bow County. The Butte Granite exhibits subvertical metamorphic foliation that is cut by 20- to 40-cm-wide aplite and pegmatite dikes. (F) Hornblende diorite sill exposed near the base of the gabbro laccolith on Bull Mountain. Photos by Kaleb Scarberry.

of about 800 km^2 (Hammarstrom, 1982; Murphy and others, 2002). The Uphill Creek Granodiorite is the largest pluton and accounts for about 75% of the batholith area. The plutons range in composition from mafic gabbro to felsic quartz monzonite and granite, and the mafic plutons are typically older than felsic plutons (Hammarstrom, 1982; Snee, 1982; Zen, 1996). Lonn and McDonald (2004) observed that tonalite (quartz diorite) is gradational to orthogneiss in the batholith. K/Ar (biotite, hornblende), $^{40}Ar/^{39}Ar$ (biotite, muscovite), and U-Pb (zircon) radiometric ages for the Pioneer Batholith range from about 80 Ma to about 64 Ma, with the younger ages likely recording post-intrusive cooling (Zen and others, 1975; Snee, 1978, 1982; Marvin and others, 1983; Lund and others, 2007).

Philipsburg Batholith

The Philipsburg Batholith consists of two plutons that cover an area of 120 km^2 between Missoula and Butte (fig. 1). The plutons create an aureole of hornblende–hornfels facies metamorphism where they are in contact with Proterozoic–Mesozoic metasedimentary and sedimentary rocks. Hyndman and others (1982) divided the batholith into two principal plutons, the smaller quartz–diorite Bimetallic stock to the west and the larger quartz–monzonite Dora Thorn pluton to the east. Hyndman and others (1972, 1982) and Naibert and others (2010) reported that the Philipsburg Batholith formed between 77 and 72 Ma based on K-Ar ages of hornblende and biotite, with crystallization of the Bimetallic stock preceding that of the Dora Thorn pluton. However, Naibert and others (2010) found no significant age difference between the Bimetallic stock and Dora Thorn pluton and reported that emplacement of the entire batholith occurred during a 0.5 million year period, at about 75 Ma ($^{40}Ar/^{39}Ar$ age of biotite). The eastern edge of the Dora Thorn pluton has younger apparent ages of 65 to 74 Ma ($^{40}Ar/^{39}Ar$ age of biotite) that may record partial resetting of the $^{40}Ar/^{39}Ar$ system in biotite during emplacement of the adjacent, and younger, Mount Powell Batholith (Marvin and others, 1989; Naibert and others, 2010). Contact-metamorphic replacement deposits and lode veins, including the extremely productive Granite–Bimetallic lode, formed during emplacement of the Philipsburg Batholith (Emmons and Calkins, 1913).

Mount Powell Batholith

The Mount Powell Batholith, located between Philipsburg and Butte (fig. 1), consists of several plutons that cover an area of roughly 300 km^2. The batholith is a complex of monzogranitic to monzodioritic plutons, sills, and dikes, as well as interlayered sheets of strongly foliated quartz–chlorite–biotite phyllite, quartz–muscovite schist, and quartz–feldspar–chlorite–epidote gneiss (Elliott and others, 2013). Many of these rocks were mapped as altered diorite by Mutch (1960, 1961) and were later reinterpreted as deformed metasedimentary inclusions that predate the batholith (Elliott and others, 2013). The Mount Powell Batholith formed between about 68 and 59 Ma (Baty, 1973; Marvin and others, 1989; Grice, 2006). Based on scattered apatite fission-track dates (70.8 to 50.7 Ma; Baty, 1973) and regional trends in apparent emplacement ages, Naibert and others (2010) argued that emplacement of the Mount Powell Batholith is likely younger than 65.4 Ma and that existing radiometric ages were affected by emplacement of the adjacent Philipsburg Batholith (fig. 1). Naibert and others (2010) also note that more geochronologic data are needed to explain existing age distributions. Elliott and others (2013) noted that the Mount Powell Batholith crystallized before about 53 Ma (Foster and others, 2010), when it was cut by detachment faults.

Tobacco Root Batholith

The 300 km^2 Tobacco Root Batholith is the largest satellite pluton of the Boulder Batholith and is the only significant pluton emplaced east of the leading edge of the fold-thrust belt. The Tobacco Root Batholith intrudes Archean basement rocks and consists of a granite core that zones outward to hornblende diorite and an alkalic layered mafic intrusion (Lady of the Lake pluton). Reported ages range from 77 to 75 Ma (Mueller and others, 1996; Sarkar and others, 2009).

Big Belt Plutons

The Big Belt plutons are satellite intrusions to the Boulder Batholith and are exposed over an area of about 600 km^2 east of Helena (fig. 1; Tilling, 1973). The two primary masses are quartz monzodiorite and a weakly developed mafic border phase that forms the northwest-trending crest of the Big Belt Mountains. These plutons formed during a single magmatic event (du Bray and Snee, 2002), with zircon U-Pb dates suggesting emplacement ca. 66.2 ± 0.9 Ma (Lund and others, 2002). Gold placer workings, including those in Confederate Gulch where 6 to 18 million dollars' worth of gold (valuation as of 1933) was produced before 1933 (Lyden, 1948), are likely derivatives of an intrusion-related gold system that formed during crystallization of the quartz monzodiorite (du Bray and Snee, 2002).

Others

Isolated 120 Ma to 70 Ma granodiorites, as well as 105 Ma syenite plutons, are mapped in northwestern Montana (Marvin and others, 1984; Harrison and others, 1986), a region of the State that remains largely understudied. Numerous smaller plutons are scattered throughout southwestern Montana, but are not addressed in detail here. The reader is referred to Foster and others (2007) for additional details about the smaller, more obscure plutons.

VOLCANIC DEPOSITS

Stratovolcanoes formed along the length of the North American Cordillera (fig. 1) during Mesozoic arc magmatism, distributing lavas, ash-flow tuffs, and air-fall deposits along their margins and into adjacent basins (Yonkee and Weil, 2015). In Montana, a volcanic belt established itself west of the Western Interior Seaway (fig. 2) during the Late Cretaceous (Robinson Roberts and others, 1995). The products of Mesozoic volcanic activity include volcanic fields, epiclastic volcanic deposits, and bentonite beds that are interstratified with fine-grained marine sediments (figs. 4, 5). Epiclastic deposits (fig. 6) are dominantly volcanic rock fragments produced during eruptions and reworking of volcanic deposits by surface processes. Collectively, the volcanic deposits record the formation, uplift, and erosion and sedimentary redistribution of rocks that composed a broad Mesozoic volcanic plateau (fig. 7).

Volcanic Fields and Successions

Volcanic deposits are notorious for their significant lateral variation in thickness and texture, which makes them difficult to correlate regionally with much certainty, although an attempt at correlating volcanic deposits in Montana from published studies is made here (fig. 7). Primary volcanic deposits include basaltic andesite lava flows and breccia, water-lain tuff, rhyolite tuff and breccia, rhyolite–dacite ignimbrites, and dacite lavas and flow domes. The best exposures of these volcanic rocks occur in the Adel Mountain Volcanics (AMV), the Bannack volcanic succession, the Elkhorn Mountains Volcanics (EMV), and at Sliderock Mountain volcano (figs. 1, 6). Epiclastic volcanic deposits including reworked tuff, mudflows, and isolated channels of volcanic sands and conglomerate are interstratified with the volcanic fields.

The Adel Mountain Volcanics

The AMV cover about 900 km^2 and are incised by the Missouri River between Great Falls and Helena (fig. 1). The remnants of at least one eroded stratovolcano occur in the AMV (Lyons, 1944), which consists of about 1,000 m of basaltic andesite lavas (fig. 7), intercalated breccia, and volcaniclastic sediments. Numerous plugs and sills and thousands of high-potassium mafic dikes intrude the lava succession (Harlan and others, 2005). Dikes exhibit radial patterns outward from plugs and stocks and connect to laccoliths north and east of the volcanic field (Hyndman and Alt, 1987). The AMV formed over a 2 to 3 million year period, from about 76 to 73 Ma (Harlan and others, 2005).

The Bannack Volcanic Field

Volcanic rocks and related intrusions of the Bannack volcanic field cover 160 km^2 and define a north–south-trending belt south of the Pioneer Batholith southwest of Dillon (Lowell, 1965; Ruppel and others, 1993). These rocks are informally referred to as the Bannack volcanic field (fig. 1). Volcanic intervals are intercalated with sediments of the synorogenic Beaverhead Group (Johnson, 1986; Azevedo, 1993), which together rest on an unconformity and lie above deformed Paleozoic formations. Extensive subvolcanic intrusions crystallized during the waning stages of volcanism (Thomas, 1981; Kalakay, 2001). The Bannack volcanic succession consists of four discrete intervals, listed oldest to youngest: (1) a 79 Ma andesitic ash-flow tuff (Murphy, 2000), which underlies coarse sedimentary deposits of the lower Beaverhead Group; (2) the 73 Ma Grasshopper Creek tuff (Mosolf, 2019), which rests conformably on the lower Beaverhead Group and contains pyroclastic flow deposits (Pearson and Childs, 1989); (3) the Cold Spring Creek volcanic deposits, which erupted from 73 to about 72 Ma (Ivy, 1988; Mosolf, in review, a,b), consisting of a complex, intertonguing succession of vent-proximal volcanic breccia, dacitic lava flows, ash-flow deposits, and volcaniclastic sediment; and (4) a 71 Ma dacite flow-dome complex and numerous 73 to 71 Ma diorite–granodiorite intrusions, including the McDowell Springs intrusive sheet and the Bannack and Anniversary plutons. Extensive gold-bearing orebodies occur near the contact between Late Cretaceous intrusions

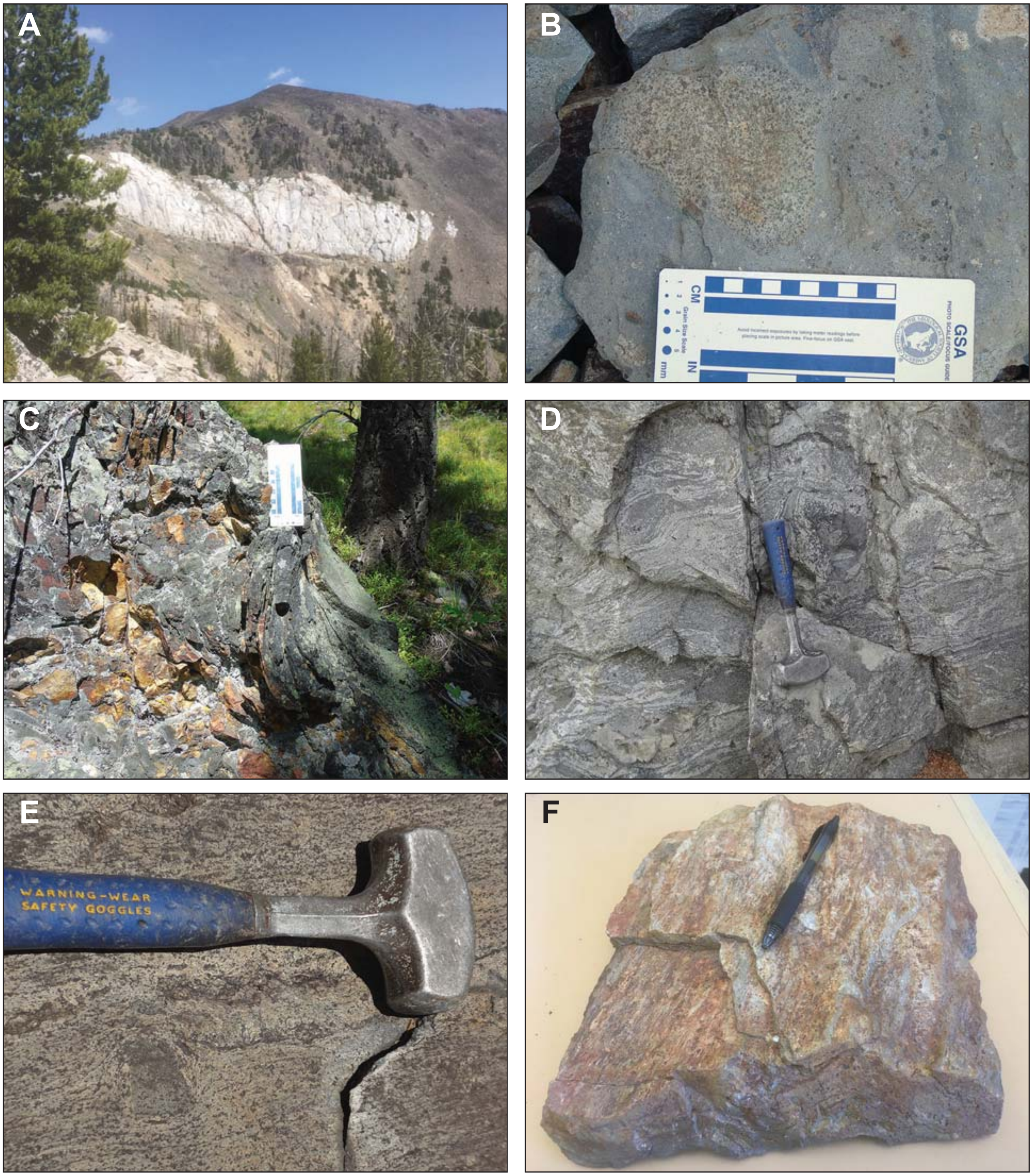

Figure 5. Mesozoic extrusive rocks. (A) Selvedge of marble more than 30 m thick that is incorporated into the lower and middle member of the Elkhorn Mountains Volcanics (EMV) on Windy Ridge, located immediately southwest of Elkhorn Peak, Jefferson County. (B) Lag breccia formed during caldera collapse and eruption of the middle member EMV near MacDonald Pass, Lewis and Clark County. (C) Ramp structures in autobrecciated rhyodacite flow-domes of the lower member EMV in the Little Blackfoot River drainage, Powell County. (D) Rheomorphic flow fabric in middle member ignimbrite of the EMV on Bull Mountain, Jefferson County. (E) Pyroclast in flow-banded middle member ignimbrite of the EMV on Bull Mountain. (F) Rock from the base of a middle member ignimbrite of the EMV south of Boulder, Jefferson County. This rock sample exhibits features formed during simple shear, including sheath folds (cross-section) and stretching lineations (aligned with pen in photo) that indicate bidirectional flow of the pyroclastic density current or ignimbrite. Photos by Kaleb Scarberry.

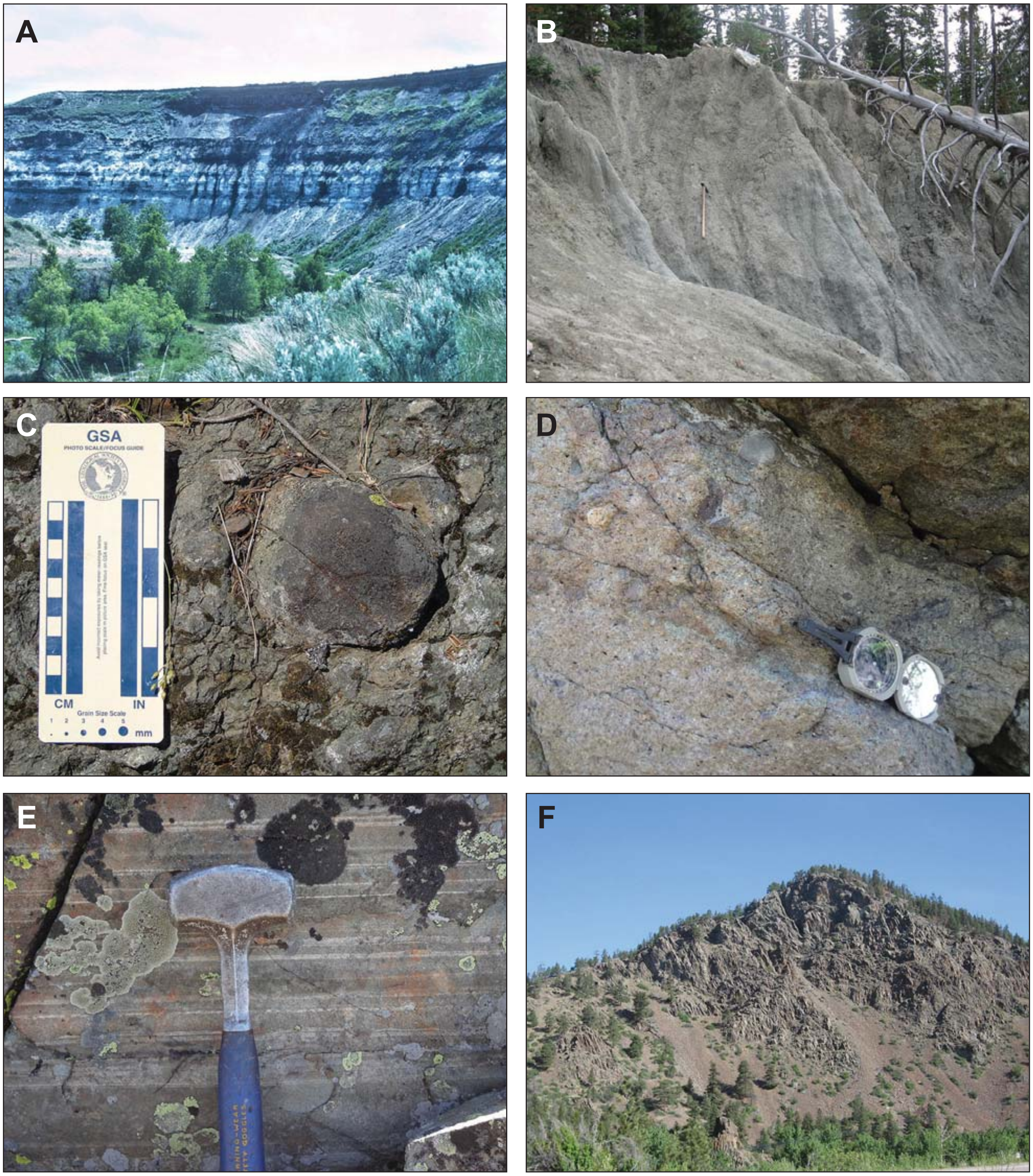

Figure 6. Mesozoic volcaniclastic deposits. (A) Chemically weathered volcanic ash or bentonite beds interbedded with marine shale of the Marias River Shale, Kevin Member, Chouteau County. The ash in the beds formed during pyroclastic ignimbrite eruptions of the middle member Elkhorn Mountains Volcanics (EMV). (B) Bentonitic mudstone of the Blackleaf Formation, Vaughn Member, Gallatin County. (C) Andesite fluvial cobble, perhaps mobilized and deposited during a lahar in the EMV sequence, Little Blackfoot River drainage, Powell County. (D) Subrounded to subangular rip-up pebbles of pre-Mesozoic rocks in upper member(?) ignimbrite of the EMV east of Deer Lodge, Deer Lodge County. (E) Water-lain ash and lapilli tuff beds near the top of the middle member EMV on the southern end of Bull Mountain, Jefferson County. (F) Volcanic member of the Two Medicine Formation near Wolf Creek, Lewis and Clark County. A, B, F: photos by Susan Vuke; C, D, E: photos by Kaleb Scarberry.

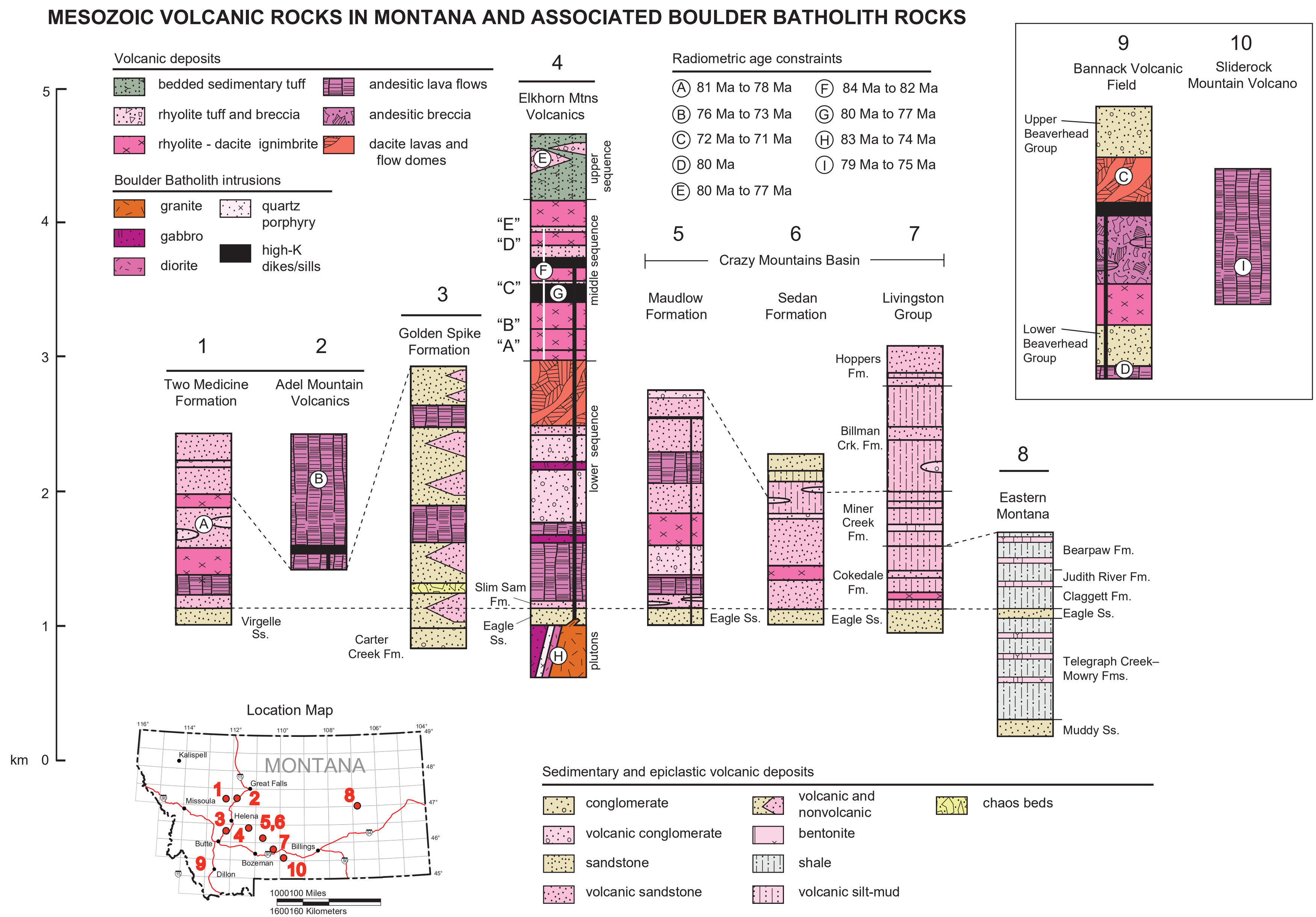

Figure 7. Composite lithostratigraphic sections. Dashed lines show reasonable age correlations based on published work: 1, Schmidt (1978); 2, Harlan and others, 2005; 3, Gwinn and Mutch (1965); 4, Schematic composite from Prostka (1966), Olson and others (2016), Becraft and others (1963), DeWitt and others (1996), Scarberry (2016b), and Korzeb and others (2018); 5 and 6, Skipp and McGrew (1977); 7, Roberts (1972); 8, Knechtel and Patterson (1956); 9, Mosolf, 2019; 10, du Bray and Harlan (1998).

and underlying Mississippian limestone (e.g., Shenon, 1931; Sassman, 1941; Geach, 1972; Pearson and Childs, 1989).

The Elkhorn Mountains Volcanic Field

The EMV form the largest Mesozoic volcanic field in Montana and were first described by Klepper and others (1957) in the Elkhorn Mountains, east of Helena. These rocks are exposed regionally over an area greater than 25,000 km^2, which includes both flanks and roof pendants to the Boulder Batholith (fig. 1). The EMV were originally up to 4.6 km thick (Tilling and others, 1968). Together, the EMV and comagmatic Boulder Batholith represent a rare and well-preserved record of continental magmatism (e.g., Lipman, 1984). Beginning in the 1950s and into the 1970s, geologists from the U.S. Geological Survey and the Montana Bureau of Mines and Geology mapped and described much of the EMV (Robertson, 1953; Klepper and others, 1957; Ruppel, 1961, 1963; Becraft and others, 1963; Prostka, 1966; Smedes, 1966; Klepper and others, 1971b; Weeks, 1974). Precious metal and base metal ore deposits track both the western and eastern contact between the EMV and the Boulder Batholith (summaries in Scarberry and others, 2019a,b).

Smedes (1966) divided the EMV into three volcanic members (fig. 7). (1) A lower member is dominated by basaltic andesite to rhyodacite lavas and pyroclastic to epiclastic volcanic deposits. In the northern Elkhorn Mountains between Boulder and Helena, the lower member consists of about 650 m of andesitic epiclastic and volcaniclastic sedimentary deposits that are intruded by mafic sills and interstratified with andesite tuffs and amygdaloidal basaltic lavas (Smedes, 1966). (2) The middle member averages 1,650 m thick and is characterized by at least seven welded rhyolite tuff sheets intercalated with epiclastic volcanic debris derived from erosion of the lower member. Klepper and others (1971b) described 1,500 m of the middle member near Elkhorn. (3) The upper member has a maximum thickness of 600 m and is dominated by bedded and water-lain tuff, as well as andesitic epiclastic volcanic rocks (Smedes, 1966). The upper member is best exposed in roof pendants on the Boulder Batholith between Butte and Helena (fig. 1; Becraft and others, 1963; Olson and others, 2017).

Recent mapping in the EMV has focused on the age, eruptive history, and regional stratigraphic correlation of the volcanic deposits. Rhyolite tuffs on the west flank of the Boulder Batholith were mapped by Scarberry (2016a) as the middle member of the EMV, but the tuffs are intercalated with sediments and bedded tuff, are about 78 to 79 Ma (Korzeb and others, 2018), and may instead correlate with the upper EMV member (fig. 7). In the main roof pendant situated over the center of the Boulder Batholith (Becraft and others, 1963), upper member volcanic sandstones and middle member rhyolite tuffs are crosscut by 83 Ma granite porphyry intrusions (Olson and others, 2017). High-potassium dikes and sills (fig. 4) intruded the EMV (fig. 7) between about 80 and 77 Ma (DeWitt and others, 1996; Olson and others, 2016; Scarberry, 2016b).

The middle member of the EMV is best exposed on the eastern margin of the Boulder Batholith where it was deposited ca. 82 to 84 Ma (Olson and others, 2016). Scarberry and others (2019a) correlated middle member rhyolite tuffs along the eastern flank of the Boulder Batholith using stratigraphic nomenclature developed by Prostka (1966). Three of these rhyolite tuffs (A, B, and C; fig. 7) are regionally extensive rheomorphic ignimbrites that have a minimum volume of 200–400 km^3 each; rheomorphic flow indicators show NNE–SSW and E–W movement of the units as they cooled (Scarberry and others, 2016). Most vents for the ignimbrite field are probably lost to erosion. Vent-proximal deposits have been described on the western flank of the Boulder Batholith, where Scarberry (2016a) mapped the contact between lower member andesitic lavas and middle member rhyolite tuff and tuff breccia as a caldera wall unconformity. Vent-proximal rhyolite deposits occur along the eastern flank of the Boulder Batholith (DeWitt and others, 1996; Olson and others, 2016).

Sliderock Mountain Volcano

The Sliderock Mountain volcano is located between Bozeman and Billings (fig. 1) along the southern margin of the Crazy Mountains Basin. Weed (1893) described the volcano as a series of northwest-trending vents, small stocks, dikes, lava flows, and volcaniclastic rocks exposed over an area of about 120 km^2. The volcanic pile is about 1,000 m thick and consists of basaltic andesite lava flows, minor intercalated pyroclastic deposits and epiclastic volcanic sediments of the Livingston Group, clast-supported lahar deposits, and porphyritic basaltic andesite lava flows (fig. 7; du Bray and others, 1994). The oldest lavas at the Sliderock Mountain volcano overlie Mesozoic sedimentary rocks and erupted at about 78 Ma. Dikes that crosscut all other units crystallized at about 75 Ma (du Bray and Harlan, 1998).

Epiclastic Volcanic Deposits

Epiclastic volcanic deposits occur outward of the volcanic fields, mainly east of but also within the Helena structural salient (fig. 1), where they are interstratified with lavas and tuffs. Almost all epiclastic successions rest with slight unconformity over Upper Cretaceous marine sandstone and conglomerate (fig. 7) of the Virgelle Sandstone in western Montana and the Eagle Sandstone in central and eastern Montana (see Vuke and others, 2007). Continental epiclastic successions become increasingly fine-grained and water-lain from west to east (fig. 7), reflecting a change from continental deposition to coastal and marine deposition within the Western Interior Seaway (fig. 7).

Two Medicine Formation

The Two Medicine Formation consists of two laterally separate deposits that are age-equivalent to the AMV: (1) the eastern facies, which is mainly sedimentary rock, and (2) the western facies, which contains mostly volcanic rocks (Viele and Harris, 1965). Only the western facies of the Two Medicine Formation is discussed here. The western facies averages about 1,000 m thick and is composed of a lower sedimentary member and an upper volcanic member (fig. 7; Schmidt, 1978). The sedimentary member formed in a continental to brackish water setting (Schmidt, 1978) and conformably overlies the Virgelle Sandstone. Material from both the EMV and the AMV likely contributed to the volcanic member of the Two Medicine Formation. A 200-m-thick section of welded dacite ignimbrite is interstratified with epiclastic volcanic siltstone to conglomerate, as well as bentonite in the bottom part of the volcanic member. $^{40}Ar/^{39}Ar$ ages of plagioclase, biotite, and sanidine in the bentonite beds range from 81 to 78 Ma (King, 1997; Roberts and Hendrix, 2000; Foreman and others, 2008), which are similar in age and composition to those of the EMV. The upper part of the volcanic member of the Two Medicine Formation (fig. 6F) contains basaltic to andesitic clasts that are similar in composition to the AMV.

Golden Spike Formation

The Golden Spike Formation (Gwinn, 1961; Gwinn and Mutch, 1965) is a unique succession of epiclastic volcanic sediment, a mixture derived from uplifted sedimentary strata sourced from the west and coarse to fine epiclastic volcanic debris and EMV lavas sourced from the east. The formation is 2,000 m thick (fig. 7) and is exposed over a northwest-elongate area of about 70 km^2 between Helena and Philipsburg (fig. 1). The nonvolcanic base of the succession is texturally and compositionally immature conglomerate and sandstone. Gwinn and Mutch (1965) described “chaos beds” low in the section (fig. 7) that contain mixed nonvolcanic and volcanic blocks 10–15 m long and set in a volcanic matrix. The chaos beds are thought by Gwinn and Mutch (1965) to record rapid introduction of material from a nearby, high-relief source. Clasts in the deposit include rounded cobbles of Mesoproterozoic Belt Supergroup rocks, Paleozoic carbonates, and angular blocks of Mesozoic sandstone and volcanic rocks (Gwinn and Mutch, 1965; Mackie, 1986; Waddell, 1997). The chaos beds likely represent a sector collapse deposit (e.g., Tilling, 2000) that originated from the west-facing flank of an EMV stratovolcano. The EMV is located about 15 km east of the chaos beds, and when the debris flow swept westward, it plucked large, angular, nonvolcanic blocks from rock ledges to the west (Sears and others, 2010). A series of dominantly andesitic lavas and flow breccia interbedded with epiclastic volcanic debris forms the top of the succession in the southeastern part of the exposure. The Golden Spike Formation lacks pyroclastic debris (Gwinn and Mutch, 1965), suggesting that it may correlate with the lower, mostly effusive, andesitic member of the EMV (fig. 7).

Slim Sam Formation

The Slim Sam Formation (Klepper and others, 1957) occurs locally at the base of the EMV and is exposed along the northeast flank of the Boulder Batholith between Boulder and Helena (Klepper and others, 1971b; Tysdal, 2000). Erosional debris from the earliest units of the EMV occurs in the Slim Sam Formation, indicating that these deposits record the transition from marine-dominated sedimentation to continental epiclastic sedimentation, as well as the initiation of volcanism within the EMV (Klepper and others, 1957). The Slim Sam Formation averages about 300 m thick, with the bottom two-thirds consisting of marine sandstone to shale and the upper third consisting of epiclastic volcanic sedimentary rocks (Smedes, 1966). The formation is not recognized south and west of the Boulder–Helena region (Klepper and others, 1957). The Slim Sam Formation might be the oldest and westernmost tongue of Livingston Group andesitic sediments, according to Klepper and others (1957).

Livingston Group and the Maudlow and Sedan Formations

Epiclastic volcanic sedimentary rocks filled the actively subsiding Crazy Mountains Basin (fig. 1) with 4,000 m of material derived principally from the EMV during the Late Cretaceous (Roberts, 1972). These deposits were originally named the Livingston Formation by Weed (1893) and were later elevated to Group status by Roberts (1963). The Livingston Group is defined by deposits of epiclastic volcanic conglomerate, sand, silt, and mud, and intercalated bentonite beds and ignimbrite deposits that occur above the Eagle Sandstone (fig. 7) and below the Fort Union Formation in the Crazy Mountains Basin. The Livingston Group is split into four formations, listed from oldest to youngest: (1) the Cokedale Formation, (2) the Miner Creek Formation, (3) the Billman Creek Formation, and (4) the Hoppers Formation.

About three-quarters of the Livingston Group consists of volcanic silt and mud. These fine-grained deposits coarsen to the north and northwest where they correlate with parts of the Sedan and Maudlow Formations, respectively (fig. 7). The Sedan Formation was first referred to as the Leaf Beds by Weed (1893) because of its abundant carbon-rich plant debris. The Sedan Formation (Skipp and McGrew, 1977) is about 1,140 m thick and consists mostly of nonmarine epiclastic volcanic sandstone, mudstone, and conglomerate interbedded with small volumes of lahars, ignimbrite, bentonite, and lignite. The Sedan Formation correlates with the lower part of the Livingston Group, or the Miner Creek and Cokedale Formations of Roberts (1972), in the southern part of the Crazy Mountains Basin (Skipp and others, 1999). The rocks have primary dips of less than 5° and are the same age as their vent facies equivalents, the EMV (Skipp and McGrew, 1977). The Maudlow Formation is about 1,600 m thick and consists of epiclastic volcanic conglomerate, sandstone, and siltstone (Skipp and Peterson, 1965; Skipp and McGrew, 1977). The Maudlow Formation correlates with the lower part of the Livingston Group in the western part of the Crazy Mountains Basin (fig. 1). Dacitic welded tuffs interstratified with the epiclastic rocks resemble lower member EMV welded dacite tuffs (Smedes, 1966) and indicate that they may be aerially extensive, similar to middle member EMV rhyolite ignimbrite sheets. High-K dikes and sills intruded the Maudlow Formation and may be age-equivalent to 80 to 77 Ma high-potassium dikes and sills that intruded middle member ignimbrites in the EMV (fig. 7; Merrill, 1895; Klepper and others, 1957; Smedes, 1966; DeWitt and others 1996; Scarberry and others, 2016; Olson and others, 2016).

Bentonite Deposits

Large reserves of industrial quality bentonite are interstratified with fine-grained, largely marine shales in eastern Montana (fig. 7; Roberts, 1963; Knechtel and Patterson, 1965; Berg, 1990). Bentonite is a volcanic ash deposit that has been altered to soft, light-colored clay owing to sedimentary and chemical processes. A total of 24 bentonite beds that range in thickness from 5 cm to 15 m occur in a 1,500 m section of shale that was deposited between 96 and 75 Ma in eastern Montana (Knechtel and Patterson, 1965; Vuke and others, 2007). Bentonite beds in middle to Upper Cretaceous shales (figs. 6A, 6B) were derived from the Sierra Nevada and Idaho Batholiths (fig. 1; Christiansen and others, 1994). Latest Cretaceous bentonite beds in the Claggett, Judith River, and Bearpaw Formations in eastern Montana, on the other hand, correlate with Late Cretaceous volcanic fields and epiclastic deposits in western and central Montana (fig. 7; Skipp and McGrew, 1977). Mesozoic sediments in western Montana also contain bentonite deposits (e.g., Walker, 1987; Roberts and Hendrix, 2000; Foreman and others, 2008), but they are not as extensive as those in eastern Montana.

DISCUSSION: MESOZOIC MAGMATISM IN MONTANA

Batholiths and plutons in Idaho and Montana (fig. 1) have long been considered products of Cordilleran arc magmatism (e.g., Dickinson, 1970; Rutland and others, 1989; Saleeby and others, 1992; Lee and others, 2007; Gaschnig and others, 2011). Subduction and back-arc, or foredeep (fig. 8), magmatism in most Cordilleran volcanic arcs involves mixing of crustal and mantle melts to generate calc-alkaline intrusions (e.g., du Bray and Snee, 2002). In Idaho and Montana, progressive crustal thickening culminated in a Late Cretaceous shift from metaluminous [wt.% Al_2O_3 < (CaO + Na_2O + K_2O)] to peraluminous [wt.% Al_2O_3 > (CaO + Na_2O + K_2O)] mantle-derived melts and triggered

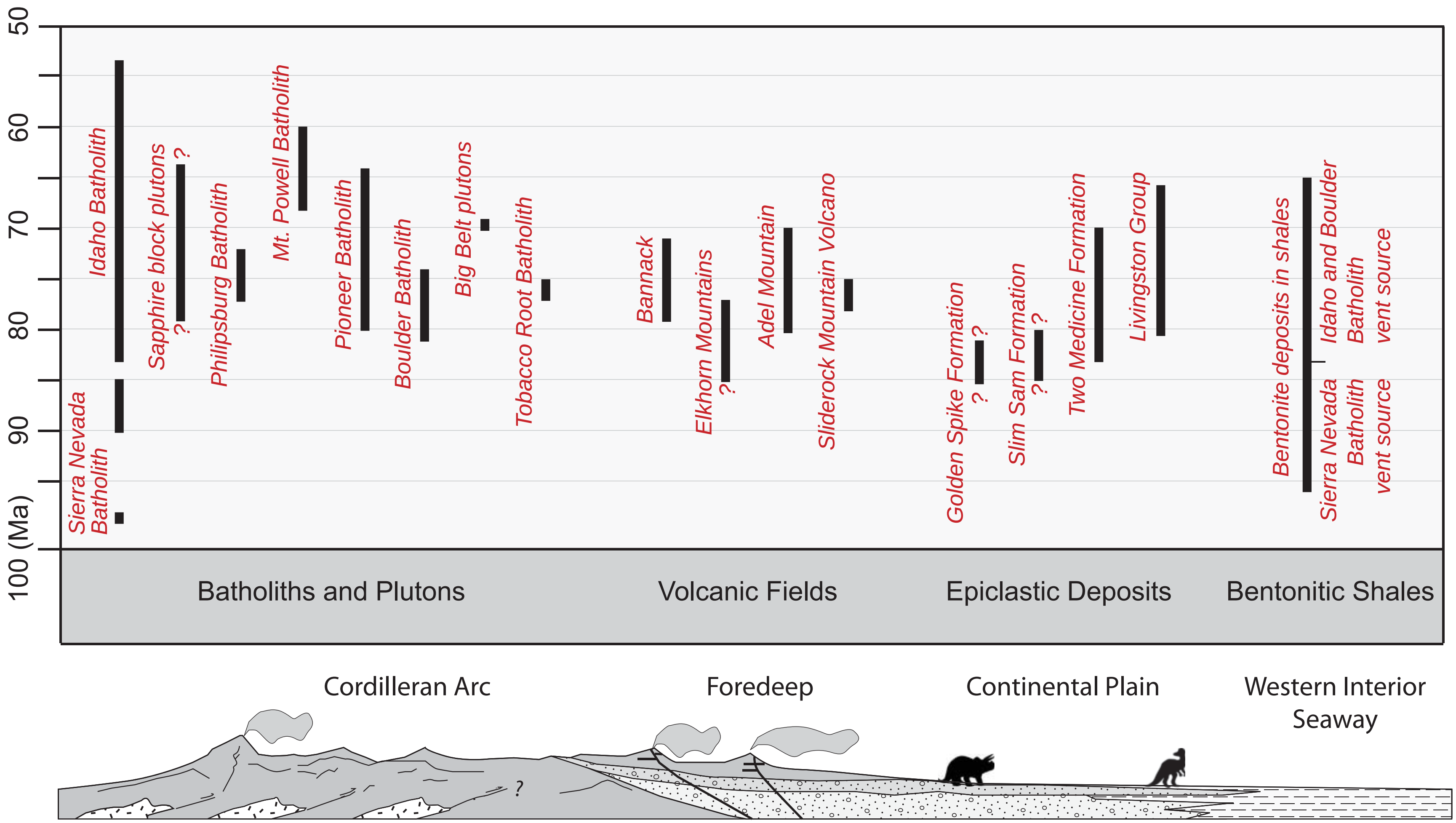

A schematic representation of the Mesozoic magma system in Montana.

Figure 8. Duration of Mesozoic magmatism and volcanism and a highly generalized cartoon of the Mesozoic Cordilleran arc in Montana. Note that no direct correlation between individual Mesozoic igneous systems and their tectonic setting depicted in the cartoon is implied here. Note that deposit types are arranged by longitude with respect to one another (e.g., Bannack is the westernmost volcanic field), but not with respect to other deposit types (e.g., the Adel Mountain volcanic field occurs at a similar longitude as the Two Medicine Formation). Emplacement/eruption ages of different igneous units are based on references cited throughout the main text.

crustal melting of Proterozoic rocks (e.g., Mueller and others, 1996; Sarkar and others, 2009; Gasching and others, 2011; du Bray and others, 2012; Foster and others, 2012). The shift in melt composition is significant because it is independent of lithology and instead records changes in pressure, temperature, and water content within the crustal melt zone (Conrad and others, 1988). Hildebrand (2013) and Hildebrand and Whalen (2017) argued that the rapid change in late melt composition, from metaluminous to peraluminous, was a precursor to the initiation of early Eocene slab failure and rollback in Montana (e.g., Copeland and others, 2017) and throughout the North American Cordillera (fig. 1).

Magma Generation

Most Mesozoic batholiths in Montana have a mafic border phase consisting of smaller volumes of alkalic plutons. The Boulder, Pioneer, and Tobacco Root Batholiths (fig. 1) all contain minor amounts of alkalic, ultramafic to mafic rocks that are thought to represent early phases of the batholiths themselves. Border phase plutons in the Boulder Batholith crystallized from melts that fractionated plagioclase, clinopyroxene, hornblende, titanite, apatite, and magnetite (du Bray and Snee, 2002; du Bray and others, 2012). Compositional variability among mantle-derived mafic border phase plutons in the Tobacco Root Batholith is explained by fractional crystallization of olivine and pyroxene, with minor amounts of crustal assimilation (Sarkar and others, 2009).

Mesozoic volcanic rocks show evidence of both crustal assimilation and fractional crystallization during their evolution. Rocks in the EMV field are generally high in alkalis (K and Na) and are metaluminous and calc-alkaline (Rutland and others, 1989). Mafic to intermediate composition rocks are relatively enriched in large ion-lithophile elements (K, Rb, Sr, Cs, Ba, Rb) and Pb, which suggests assimilation of crustal rocks during crystallization. Silicic compositions are variably depleted in Sr, P, Ti, Nb, Ta, and the middle rare earth elements (Sm, Eu, Dy), which could reflect minor crystal fractionation of plagioclase, apatite, amphibole, and spinel (Olson and others, 2016). In the Bannack volcanic field, the rocks are calc-alkaline, enriched in incompatible elements (Ivy, 1988), and contain abundant 2.7–1.8 Ga zircon xenocrysts (Mosolf, 2019). The presence of old zircons indicates that the parental melts assimilated evolved crustal rocks, such as crystalline basement rocks exposed in the cores of nearby folds (Coryell, 1983; Mueller and others, 2012).

Pluton Emplacement

Plutons and batholiths in southwestern Montana occur up to 200 km east of the Idaho Batholith and represent the easternmost exposures of Mesozoic Cordilleran igneous rocks in the United States (fig. 1). The distribution of plutons and batholiths sparked debate about whether they had moved considerably after crystallization (an allochthonous origin; e.g., Tilling and others, 1968; Hyndman and others, 1975; Roberts and Hendrix, 2000; Lageson and others, 2001; Foster and others, 2010; Sears, 2016), or had more or less formed where they are now (an autochthonous origin; Rutland and others, 1989; Berger and others, 2011; Houston and Dilles, 2013). The idea that slab failure (e.g., Hildebrand and Whalen, 2017) produced batholiths and plutons via partial melting of the crust appears to be consistent with both allochthonous and autochthonous origins.

Paleomagnetic data are somewhat ambiguous on the issue of allochthonous vs. autochthonous origins for the plutons and batholiths in Montana. Different data sets seem to contradict one another. For example, ca. 75 Ma mafic dikes emplaced in the AMV and the Tobacco Root Batholith region, respectively, within and east of the fold-thrust belt (fig. 1), have not experienced measurable tilting or vertical axis rotation since their emplacement (Diehl, 1991; Gunderson and Sheriff, 1991; Harlan and others, 2008a,b). In contrast, diorite sills emplaced in the Lombard thrust region (fig. 1) at 77 Ma formed contemporaneously with the AMV located about 80 km to the north–northwest (fig. 1), crystallized prior to folding, and were later deformed within northeast- and northwest-plunging folds (Harlan and others, 2008a). Together, these data suggest that some parts of the Late Cretaceous magmatic complex in Montana were deformed post-emplacement, whereas other parts were not.

Arguments for an allochthonous origin

Based primarily on the distribution of Cretaceous plutons and thrust sheets, as well as deformed rocks exposed by Paleogene detachment faults in western Montana (fig. 1), some workers have proposed that the Boulder Batholith, as well as other plutons in the Montana fold-thrust belt, slid eastward from the carapace of the Idaho Batholith (fig. 1). In this model, an east-tapering Cordilleran magma wedge (Hyndman and others, 1975; Sears, 2016) moved eastward between about 100 and 75 Ma (Sears, 2016). Subsequent extensional collapse of the Cordillera in Montana closely trailed a 65 to 53 Ma regional decompression-related crustal melting event and unroofed several metamorphic core complexes along detachment faults (Foster and others, 2001). The eastern edge of the Bitterroot lobe of the Idaho Batholith and Sapphire Block plutons are complexly deformed and characterized by intense cataclasite zones (Hyndman and others, 1975; Garmezy and Sutter, 1983). The largest of these zones, the Bitterroot detachment fault (fig. 1), formed between about 52 and 50 Ma (Foster and others, 2001) and marks the eastern edge of the Bitterroot lobe of the Idaho Batholith. Additional faulting along the Anaconda detachment, located 40–100 km east of the Bitterroot detachment (fig. 1), displaced the Boulder Batholith roughly 20–25 km eastward between about 53 and 39 Ma (Foster and others, 2010). The main arguments against an allochthonous origin for plutons, specifically the Boulder Batholith, in the Montana fold-thrust belt fall into two categories. (1) The center of the Boulder Batholith is located over 230 km east of the center of the Idaho Batholith. Restoring movement on detachment structures in the fold-thrust belt (fig. 1) does not convincingly place the Boulder Batholith on top of the Idaho Batholith. (2) The Idaho Batholith and Boulder Batholith have different ages and compositions. The Cretaceous–Paleogene Idaho Batholith is mainly biotite granodiorite (Foster and Fanning, 1997; Gaschnig and others, 2011), whereas the Late Cretaceous Boulder Batholith is mostly granite (summary in Houston and Dilles, 2013).

Arguments for an autochthonous, syncompressional origin

We note that some of the ideas discussed in this review of Mesozoic magmatism in Montana predate the accepted tectonics paradigm (e.g., Atwater, 1970), but they are discussed here nonetheless for completeness. Gwinn and Mutch (1965) said that “forceful” intrusion of the Late Cretaceous Boulder Batholith near Garrison, located about 50 mi west of Helena (fig. 1), created west-verging folds and shear zones. Woodward (1986) noted that mineral vein orientations and other structures in the Boulder Batholith are consistent with an east-directed Late Cretaceous compressional stress regime. Schmidt and others (1990) proposed that the main mass of the Boulder Batholith was emplaced along a pull-apart segment within a thin-skinned thrust sheet during east–northeast translation in the fold-thrust belt. Northwest-striking faults crosscut contractional structures of the fold-thrust belt along the east and south margins of the Boulder Batholith that may have acted as structural controls for mafic border phase pluton emplacement (Berger and others, 2011). Lageson (2001) proposed that emplacement of the Boulder Batholith, perhaps via mid-crustal channel flow (Lageson and others, 2019), thickened the fold-thrust belt orogenic wedge to the degree at which it exceeded its critical taper and reactivated preexisting thrust faults in the Helena embayment (fig. 1). Based on structural relationships, Kalakay and others (2001) argued that the Boulder and Pioneer Batholiths formed as composite tabular bodies and intruded ramps in the thrust wedge, at crustal depths of 1 to 10 km. Reverse faults may have displaced the eastern edge of the Boulder Batholith by 1–3 km after it was emplaced (Tilling and others, 1968; Smedes, 1973).

Arguments for an autochthonous, post-compressional origin

Other workers have argued that plutons and batholiths in Montana formed where they are and then were exhumed during Laramide-style deformation. Upper Cretaceous synorogenic strata of Beaverhead Group sediments in southwestern Montana and adjoining parts of Idaho are thought to record the early onset of Laramide-style deformation in Montana (Garber and others, 2020). Near Dillon, the upper Beaverhead Group is younger than about 71 Ma (fig. 7). The Boulder Batholith at Butte was emplaced after fold-thrust belt folding and was uplifted during shortening between about 66 and 61 Ma (Rutland and others, 1989; Houston and Dilles, 2013). Undeformed granite intruded folded and sheared rocks of the EMV along its eastern contact between Butte and Helena (Houston and Dilles, 2013). From north to south, the eastern margin of the Boulder Batholith cuts up-section through gently deformed Mesoproterozoic Belt Supergroup–Late Cretaceous EMV strata of a broad north-plunging anticline (Scarberry and others, 2019a). Recent geologic mapping along the eastern margin of the Boulder Batholith documented aplite sills in the Butte Granite cutting EMV volcanic foliation at 5° to 10° angles (Olson and others, 2016, 2017; Scarberry, 2016b; Scarberry and others, 2017, 2019a).

Batholith Geometry

The geometry of Mesozoic plutons and batholiths in western Montana has been the subject of considerable debate for nearly 100 years (Lawson, 1914; Hamilton and Myers, 1967, 1974; Klepper and others, 1971a, 1974; Schmidt and others, 1990). Early field studies produced two competing ideas regarding the position and geometry of the Boulder Batholith floor. One group of workers envisioned the Boulder Batholith as a thin, near-surface laccolith-like mass (Weed, 1901; Knopf, 1914; Lawson, 1914), whereas others imagined a wedge-shaped batholith mass that extended to great depths (Billingsley, 1916; Grout and Balk, 1934). Hamilton and Myers (1967) proposed that all batholiths, including the Boulder Batholith, were thin, rootless, and variable only in their differing levels of exposure.

Original thickness estimates for batholiths in southwestern Montana range from about 5 to 22 km. Hamilton and Myers (1974) argued that the Boulder Batholith crystallized at a shallow depth and is about 5 km thick. In contrast, Klepper and others (1971a) observed that the batholith cuts across an 11 km thickness of gently folded country rocks and its eastern margin is essentially straight for 50 km across rugged terrain. Klepper and others (1971a) concluded that the batholith was steep-sided and greater than 15 km thick. In the southern half of the Boulder Batholith, no roof is exposed, so the current thickness is a minimum, and hornblende barometry suggests an emplacement depth of about 6 to 10 km (Houston and Dilles, 2013). Considering gravity and seismic reflection data, Schmidt and others (1990) interpreted that the Boulder Batholith floor ends in a basal décollement that lies at a present depth of about 12 to 18 km (Vejmelek and Smithson, 1995; Burton and others, 1998). Houston and Dilles (2013) proposed a 15 to 22 km total emplacement thickness for the Boulder Batholith that is consistent with geophysical observations (summary in Berger and others, 2011), hornblende geobarometry, and fluid inclusion data (Roberts, 1973, 1975; Rusk and others, 2008). A gravity study modelled a 20 km thickness for the Tobacco Root Batholith (Tatum, 2015).

Volcanic Eruptions

Remnants of andesitic stratovolcanoes and dacite lava domes of the lower EMV member are preserved on the northwest flank of the Boulder Batholith (e.g., Scarberry and others, 2018, 2019b) and record the initiation of Mesozoic volcanism prior to about 84 Ma in Montana. Caldera-forming rhyolitic volcanism of the middle EMV member occurred between about 84 and 82 Ma and produced several ignimbrites that are preserved mainly on the east flank of the Boulder Batholith (Olson and others, 2016; Scarberry and others, 2019a). Rhyolite–dacite ignimbrites from the middle EMV member represent one of the largest silicic pyroclastic provinces known on Earth (Smith, 1960; Smedes, 1966; Klepper and others, 1971b). The lower and middle EMV members and many of their laterally interstratified counterparts are folded, indicating that volcanism, and some degree of erosion and deposition, occurred prior to fold-thrust belt deformation beginning at about 82 Ma.

The upper EMV member is younger than about 82 Ma (Olson and others, 2017) and consists of intercalated sediments, bedded tuff, and 78 to 80 Ma ash-flow tuff breccia deposits (Roberts and Hendrix, 2000; Korzeb and others, 2018). The tuffs are interstratified with epiclastic volcanic debris in adjacent epiclastic basins and travelled great distances along paleovalleys outward from their source vents. Aligned petrified trees and charred dinosaur bones are encased in bentonite in the Two Medicine Formation (fig. 7) and were felled by a single ignimbrite eruption at about 80 Ma (Roberts and Hendrix, 2000). These ashes occur in eastern Montana shales (figs. 6A, 7), southern Alberta (Thomas and others, 1990), and perhaps as far away as the Dakotas and Nebraska (Spivey, 1940; Gill and Cobban, 1973). The upper EMV member is roughly age-equivalent with the formation of younger Cordilleran foredeep stratovolcanoes such as the AMV and Sliderock Mountain, which formed between around 79 and 73 Ma (du Bray and Harlan, 1998; Harlan and others, 2005). Andesite–rhyolite deposits in the 79 to 71 Ma Bannack volcanic field (Mosolf, 2019) are also time-equivalent with the upper EMV member (fig. 7). Magmatism and coeval shortening near the Bannack volcanic field occurred no later than about 78 to 80 Ma (Mosolf, 2019).

Alkalic mafic sills and laccoliths, including gabbro and lamprophyre compositions, intrude the EMV and are similar in composition, but not necessarily age, to rocks in the AMV and the Sliderock Mountain volcano (fig. 7; Harlan and others, 2008a; Olson and others, 2016; Scarberry, 2016b). Mafic sills intrude the middle member of the EMV on the east flank of the Boulder

Batholith and are about 82 to 79 Ma (DeWitt and others, 1996; Olson and others, 2016; Scarberry, 2016b). On the northwestern flank of the Boulder Batholith, an 82 Ma hornblende diorite sill crosscuts the lower EMV member (Scarberry and others, 2018, 2019b).

At least three Plinian eruptions are recorded in the middle EMV member, which scattered pyroclastic debris throughout Montana and beyond (Scarberry and others, 2016). Pyroclastic material was funneled through Late Cretaceous topographic lows near vents. Rock foliations and stretching lineations (e.g., Andrews and Branney, 2011) define east–west and northeast–southwest bidirectional rheomorphic flow pathways. The lower and middle EMV members are laterally interstratified outward with regional epiclastic volcanic deposits and bentonite-bearing shale formations, which themselves are an important record of Mesozoic magmatism in Montana (fig. 7). In a general way, the Elkhorn Mountains volcanic field represents a near-vent facies of volcanism, the Maudlow Formation is a remnant of the coarse reworked alluvial facies, and the Sedan and related formations are fine-grained distal alluvial facies (fig. 7). In addition to producing sheets of welded tuff, Plinian caldera-forming ignimbrite eruptions discharged plumes of ash more than 20 km into the stratosphere that ultimately settled in beds now interstratified with Mesozoic mudstone of the great Western Interior Seaway (fig. 2; Roberts, 1963; Knechtel and Patterson, 1965; Skipp and McGrew, 1977; Christiansen and others, 1994).

Removal of the Volcanic Carapace

The EMV, by far the largest Mesozoic volcanic province in Montana, is exposed over a 25,000 km^2 region between Butte and Helena (fig. 1) and had an original estimated thickness of about 3.5–4.6 km (Tilling and others, 1968; Lageson and others, 2011). Paleorivers connected east-central Idaho with southwestern Montana in the Late Cretaceous (Garber and others, 2020). Post-magmatic uplift and erosion removed about 7 km of rock (EMV and the underlying Boulder Batholith) above the ore deposit at Butte between ~66 and 59 Ma (Houston and Dilles, 2013; Schwartz and Schwartz, 2013). Modern exposed EMV sections are less than 2 km thick along the northwestern margin of the Boulder Batholith (Scarberry and others, 2019b) and around 1 to 2 km thick along the batholith's eastern margin (Scarberry and others, 2019a). EMV rocks, including the thickest section of the upper member, average around 0.5 km thick in the main north-central roof pendant south of Helena (fig. 1; Olson and others, 2017). These observations support the following assertions related to the timing, style, and amount of volcanic material removed from the Boulder Batholith: (1) the minimum original volume of the EMV was on the order of 100,000 km^3 prior to uplift and erosion beginning at around 66 Ma; (2) as much as half of the EMV carapace, or around 50,000 km^3 of igneous material, was removed during uplift and northward tilting (10–20°) of the magma system, primarily between about 66 and 59 Ma (Houston and Dilles, 2013; Schwartz and Schwartz, 2013); (3) concurrent with elevation gain between 58 and 53 Ma, a warm and wet climate drove deep fluvial incision through the EMV–Boulder Batholith complex (Schwartz and Schwartz, 2013; Schwartz and others, 2019a).

SUGGESTIONS FOR FUTURE RESEARCH

Several fundamental questions remain for future researchers to address. In particular, the age, distribution, geometry, and emplacement history of plutons and batholiths in Montana are unresolved. For example, did Mesozoic plutons and batholiths form during contractional deformation, extensional deformation, both contractional and extensional deformation, or maybe during a slab failure event that marked the transition in style of deformation? Additionally, opportunities for student research projects that focus on correlating epiclastic successions with adjacent volcanic fields are nearly limitless. Some of the most pressing questions, and suggestions for addressing them, are outlined below.

What Is the Age and Distribution of Plutonic Rocks in the Mesozoic Fold-Thrust Belt of Northwestern Montana?

Few Mesozoic plutons are mapped in northwestern Montana (Vuke and others, 2007), an area that covers about 40,000 km^2. However, Mesozoic plutons are abundant in the fold and thrust belt of bordering regions in Idaho (Lewis and others, 2012) and Canada (Tipper and others, 1981). Future work on mapping and obtaining geochemical and radiometric age data from Mesozoic plutons in northwestern Montana would help to evaluate existing ideas about fold-thrust belt magmatism in southwestern Montana and elsewhere in the North American Cordillera (fig. 1).

How Widespread are Mesozoic Orthogneisses in the Montana Fold-Thrust Belt, and What Can They Tell Us about Pluton Generation and Emplacement?

Orthogneiss and ultra-high-pressure rocks, such as eclogite, are found in most continent–continent convergent plate boundaries (Menold and others, 2009). Current thinking suggests that these rocks formed as coherent blocks of continental crust that were subducted to mantle depths (Tabata and others, 1998; Ye and others, 2000). The northern Rocky Mountains in Idaho and Montana were the North American craton margin during the Early Cretaceous (summary in McClelland and others, 2000). Early Cretaceous juxtaposition of accreted terranes along the Cordilleran margin along a north–south-oriented crustal structure (Tikoff and others, 2001) may have provided the pressure required to produce orthogneisses in Montana. The Bitterroot detachment fault in Montana (fig. 1) exposes mid- to lower-crust, high-grade metamorphic rocks that formed during an episode of tonalite (quartz diorite) plutonism between about 75–80 Ma (Foster and others, 2001), which is roughly the same age as the Boulder Batholith. Orthogneiss in the Pioneer Batholith (fig. 1) was originally thought to be Proterozoic (Berger and others, 1983), but now is assigned a Mesozoic age. The orthogneiss is gradational to tonalite in Pioneer Batholith plutons (Ruppel and others, 1993; Lonn and McDonald, 2004). Similar rocks may be prevalent in plutons and batholiths throughout Montana. Future work on geologic mapping, specifically to locate ultra-high-pressure rocks associated with orthogneiss, radiometric age determinations, and mineral chemistry data, will help define the extent and age of Mesozoic metamorphic rocks, their pressure–temperature forming conditions, and connection to Cordilleran arc magmatism in Montana.

Can Advances in Correlating Mesozoic Volcanic Fields, Epiclastic Deposits, and Bentonite Beds in Montana (fig. 7) Help Constrain the Tectonic Setting of Pluton Emplacement, the Magnitude of Volcanism, and Deformation?

Future work to correlate middle member EMV ignimbrites and determine their volume and age progression (e.g., Prostka, 1966; Olson and others, 2016; Scarberry and others, 2017) would help to understand the generation of magmas and the associated styles and timing of magmatism. The lower member of the EMV is not dated sufficiently. Furthermore, what is the genetic relationship among the EMV, the AMV, the Bannack volcanic field, and Sliderock volcano? Are these volcanic fields (fig. 1) disconnected pieces of the same magma system, and what are their respective deformation histories?

Studies of epiclastic volcanic successions, augmented by radiometric ages and fossil information, can be used to assess deformation in the Montana fold-thrust belt. Similar studies of the epiclastic volcanic successions from Mesozoic continental plain successions (fig. 7) would help to better understand the source and duration of sedimentation, as well as the timing of subsequent deformation.

Finally, radiometric ages and geochemical studies of bentonite beds in eastern Montana would help to determine if they can be attributed to specific eruptions. If so, a model of volcanic facies (e.g., fig. 7) could be used to evaluate how reasonable the current distribution of volcanic facies is and what it implies about Mesozoic deformation in the Montana fold-thrust belt (fig. 1).

REFERENCES CITED

Albright, L.D., 2004, Historical mining districts of Montana: Montana Bureau of Mines and Geology Open-File Report 406 (CD).

Andrews, G.D.M., and Branney, M.J., 2011, Emplacement and rheomorphic deformation of a large, lava-like rhyolitic ignimbrite: Grey's Landing, southern Idaho: Geologic Society of America Bulletin, v. 123, no. 3–4, p. 725–743, doi: https://doi.org/10.1130/B30167.1

Atwater, T., 1970, Implications of plate tectonics for the Cenozoic tectonic evolution of western North America: Geological Society of America Bulletin, v. 81, no. 12, p. 3513–3536, doi: https://doi.org/10.1130/0016-7606(1970)81[3513:IOPTFT]2.0.CO;2

Azevedo, P.A., 1993, Tectono-sedimentary evolution of a Late Cretaceous alluvial fan, Beaverhead Group, southwestern Montana: Bozeman, Montana State University, M.S. thesis, 137 p., 2 sheets.

Baty, J.B., 1973, Fission track age dates from three granitic plutons in the Flint Creek Range, western Montana: Missoula, University of Montana, M.S. thesis, 37 p.

Becraft, G.E., Pinckney, D.M., and Rosenblum, S., 1963, Geology and mineral deposits of the Jefferson City quadrangle, Jefferson and Lewis and Clark Counties, Montana: U.S. Geological Survey Professional Paper 428, 101 p.

Berg, R.B., 1990, Montana's industrial minerals, *in* Industrial rocks and minerals of the Pacific Northwest: Proceedings of the 25th Forum on the Geology of Industrial Minerals, Portland, Oregon, p. 37–44.

Berger, B.R., Snee, L.W., Hanna, W., and Benham, J.R., 1983, Mineral resource potential of the West Pioneer Wilderness Study Area, Beaverhead County, Montana: U.S. Geological Survey Miscellaneous Field Studies Map MF-1585, scale 1:50,000.

Berger, B.R., Hildenbrand, T.G., and O'Neill, J.M., 2011, Control of Precambrian basement deformation zones on emplacement of the Laramide Boulder batholith and Butte mining district, Montana, United States: U.S. Geological Survey Scientific Investigations Report 2011-5016, 29 p., doi: https://doi.org/10.3133/sir20115016

Billingsley, P., 1916, The Boulder Batholith of Montana: Transactions of the American Institute of Mining Engineers, v. 51, p. 31–56.

Burchfiel, B.C., Cowan, D.S., and Davis, G.A., 1992, Tectonic overview of the Cordilleran orogen in the western United States, *in* Burchfiel, B.C., Lipman, P.W., and Zoback, M.L., eds., The Cordilleran orogen: Conterminous U.S.: Boulder, Colo., Geological Society of America, The Geology of North America, v. G-3, p. 407–479.

Burton, B., Lageson, D., Schmidt, C., Ballard, D., and Warne, J., 1998, Large magnitude shortening of the Lombard thrust system, Helena salient, Montana fold and thrust belt: Implications for reconstruction of the Belt basin: Montana Bureau of Mines and Geology Special Publication 112, p. 229–243.

Christiansen, E.H., Kowallis, B.J., and Barton, M.D., 1994, Temporal and spatial distribution of volcanic ash in Mesozoic sedimentary rocks of the Western Interior: An alternative record of Mesozoic magmatism, *in* Caputo, M.V., Peterson, J.A., and Franczyk, K.L., eds., Mesozoic Systems of the Rocky Mountain Region, USA: Rocky Mountain Section, SEPM, p. 73–94.

Coney, P.J., 1972, Cordilleran tectonics and North America plate motion: America Journal of Science, v. 272, p. 603–628.

Conrad, W.K., Nicholls, I.A., and Wall, V.J., 1988, Water-saturated and under-saturated melting of metaluminous and peraluminous crustal compositions at 10 kb: Evidence for the origin of silicic magmas in the Taupo Volcanic Zone, New Zealand, and other occurrences: Journal of Petrology, v. 29, p. 765–803.

Copeland, P., Currie, C.A., Lawton, T.F., and Murphy, M.A., 2017, Location, location, location: The variable lifespan of the Laramide orogeny: Geology, v. 45, no. 3, p. 223–226, doi: https://doi.org/10.1130/G38810.1

Coryell, J.J., 1983, Structural geology of the Henneberry Ridge area, Beaverhead County, Montana: College Station, Texas A&M University, M.S. thesis, 126 p.

Czehura, S., 2006, Butte: A world class ore deposit: Mining Engineering, v. 58, p. 14–19.

DeWitt, E., Foord, E.E., Zartman, R.E., Pearson, R.C., and Foster, F., 1996, Chronology of Late Cretaceous igneous and hydrothermal events at the Golden Sunlight gold-silver breccia pipe, southwestern Montana: U.S. Geological Survey Bulletin 2155, 48 p.

Dickinson, W.R., 1970, Relations of andesites, granites, and derivative sandstones to arc-trench tectonics: Reviews of Geophysics and Space Physics, v. 8, p. 813–860.

Dickinson, W.R., Klute, M.A., Hayes, M.J., Janecke, S.U., Lundin, E.R., McKittrick, M.A., and Olivares, M.D., 1988, Paleogeographic and paleotectonic setting of Laramide sedimentary basins in the central Rocky Mountain region: Geological Society of America Bulletin, v. 100, no. 7, p. 1023–1039, doi: https://doi.org/10.1130/0016-7606(1988)100%3C1023:PAPSOL%3E2.3.CO;2

Diehl, J., 1991, The Elkhorn Mountains revisited: New data for the Late Cretaceous paleomagnetic field of North America: Journal of Geophysical Research: Solid Earth, v. 96, no. B6, p. 9887–9894, doi: https://doi.org/10.1029/91JB00959

du Bray, E.A., and Harlan, S.S., 1998, Geology, age, and tectonic setting of the Cretaceous Sliderock Mountain volcano, Montana: U.S. Geological

Survey Professional Paper 1602, 19 p., doi: https://doi.org/10.3133/pp1602

du Bray, E.A., and Snee, L.W., 2002, Composition, age, and petrogenesis of Late Cretaceous intrusive rocks in the central Big Belt Mountains, Broadwater and Meagher Counties, Montana: U.S. Geological Survey Professional Paper 1657, 30 p., doi: https://doi.org/10.3133/pp1657

du Bray, E.A., Elliott, J.E., Van Gosen, B.S., LaRock, E.J., and West, A.W., 1994, Reconnaissance geologic map of the Sliderock Mountain area, Sweet Grass County, Montana: U.S. Geological Survey Miscellaneous Field Studies Map MF-2259, scale 1:50,000, doi: https://doi.org/10.3133/mf2259

du Bray, E.A., Aleinikoff, J.N., and Lund, K., 2012, Synthesis of petrographic, geochemical, and isotopic data for the Boulder Batholith, southwest Montana: U.S. Geological Survey Professional Paper 1793, 39 p.

Elliott, C.G., Smith, L.N., and Lonn, J.D., 2013, Geologic map of the Mount Powell 7.5' quadrangle, southwestern Montana: Montana Bureau of Mines and Geology Open-File Report 635, scale 1:24,000.

Emmons, W.H., and Calkins, F.C., 1913, Geology and ore deposits of the Philipsburg quadrangle, Montana: U.S. Geological Survey Professional Paper 78, 271 p.

Foreman, B.Z., Rogers, R.R., Deino, A.L., Wirth, K.R., and Thole, J.T., 2008, Geochemical characterization of bentonite beds in the Two Medicine Formation (Campanian, Montana), including a new $^{40}Ar/^{39}Ar$ age: Cretaceous Research, v. 29, p. 373–385.

Foster, D.A., and Fanning, C.M., 1997, Geochronology of the northern Idaho Batholith and the Bitterroot metamorphic core complex: Magmatism preceding and contemporaneous with extension: Geological Society of America Bulletin, v. 109, no. 4, p. 379–394, https://doi.org/10.1130/0016-7606(1997)109%3C0379:GOTNIB%3E2.3.CO;2

Foster, D.A., Schafer, C., Fanning, C.M., and Hyndman, D.W., 2001, Relationships between crustal partial melting, plutonism, orogeny, and exhumation: Idaho–Bitterroot batholith: Tectonophysics, v. 342, no. 3–4, p. 313–350, doi: https://doi.org/10.1016/S0040-1951(01)00169-X

Foster, D.A., Kalakay, T.J., Mueller, P.A., and Heatherington, A., 2007, Late Cretaceous granitic plutons in southwestern Montana: Northwest Geology, v. 36, p. 73–90.

Foster, D.A., Grice, W.C., and Kalakay, T.J., 2010, Extension of the Anaconda metamorphic core complex: $^{40}Ar/^{39}Ar$ thermochronology with implications for Eocene tectonics of the northern Rocky Mountains and the Boulder Batholith: Lithosphere, v. 2, no. 4, p. 232–246, https://doi.org/10.1130/L94.1

Foster, D.A., Mueller, P.A., Heatherington, A., Gifford, J.N., and Kalakay, T.J., 2012, Lu-Hf systematics of magmatic zircons reveal a Proterozoic crustal boundary under the Cretaceous Pioneer Batholith, Montana: Lithos, v. 142–143, p. 216–225, doi: https://doi.org/10.1016/j.lithos.2012.03.005

Foster, F., and Childs, J.F., 1993, An overview of significant lode gold systems in Montana, and their regional geologic setting: Exploration Mining Geology, v. 2, p. 217–244.

Gammons, C.H., Korzeb, S.L, and Hargrave, P.A., 2020, Metallic ore deposits of Montana, *in* Metesh, J.J., and Gammons, C.H., eds., Geology of Montana—Special Topics: Montana Bureau of Mines and Geology Special Publication 122, v. 2, 30 p.

Garber, K.L., Finzel, E.S., and Pearson, D.M., 2020, Provenance of synorogenic foreland basin strata in southwestern Montana requires revision of existing models for Laramide tectonism: North American Cordillera: Tectonics, 26 p., doi: https://doi.org/10.1029/2019TC005944

Garmezy, L., and Sutter, J.F., 1983, Mylonitization coincident with uplift in an extensional setting, Bitterroot Range, Montana-Idaho: Geological Society of America Abstracts with Programs, v. 15, p. 578.

Gaschnig, R.M., Vervoort, J.D., Lewis, R.S., and Tikoff, B., 2011, Isotopic evolution of the Idaho Batholith and Challis Intrusive Province, northern US Cordillera: Journal of Petrology, v. 52, no. 12, p. 2,397-2,429, doi: https://doi.org/10.1093/petrology/egr050

Geach, R.D., 1972, Mines and mineral deposits (except fuels), Beaverhead County, Montana: Montana Bureau of Mines and Geology Bulletin 85, 194 p., 3 sheets.

Gill, J.R., and Cobban, W.A., 1973, Stratigraphy and geologic history of the Montana Group and equivalent rocks, Montana, Wyoming, and North and South Dakota: U.S. Geologic Survey Professional Paper 776, 37 p.

Grice, W.C., Jr., 2006, Exhumation and cooling history of the middle Eocene Anaconda Metamorphic Core Complex, western Montana: Gainesville, University of Florida, M.S. thesis, 261 p.

Grout, F.F., and Balk, R., 1934, Internal structures in the Boulder Batholith: Geological Society of America Bulletin, v. 45, no. 5, p. 877–896, doi: https://doi.org/10.1130/GSAB-45-877

Gunderson, J.A., and Sheriff, S.D., 1991, A new Late Cretaceous paleomagnetic pole from the Adel Mountains, west central Montana: Journal of Geophysical Research, v. 96, no. B1, p. 317–326, doi: https://doi.org/10.1029/90JB01963

Gwinn, V.E., 1961, Geology of the Drummond area, central-western Montana: Montana Bureau of Mines and Geology Geologic Map 4, 1 sheet, scale 1:63,360.

Gwinn, V.E., and Mutch, T.A., 1965, Intertongued Upper Cretaceous volcanic and nonvolcanic rocks, central-western Montana: Geological Society of America Bulletin, v. 76, no. 10, p. 1125–1144, doi: https://doi.org/10.1130/0016-7606(1965)76[1125:IUCVAN]2.0.CO;2

Hamilton, W.B., 1988, Laramide crustal shortening, *in* Schmidt, C.J., and Perry, W.J., Jr., eds., Interaction of the Rocky Mountain Foreland and the Cordilleran Thrust Belt: Geological Society of America Memoir 171, p. 27–39.

Hamilton, W., and Myers, W.B., 1967, The nature of batholiths: U.S. Geological Survey Professional Paper 554-C, 30 p., doi: https://doi.org/10.3133/pp554C

Hamilton, W., and Myers, W.B., 1974, The nature of the Boulder Batholith of Montana: Geological Society of America Bulletin, v. 85, p. 365–378.

Hammarstrom, J., 1982, Chemical and mineralogical variation in the Pioneer Batholith, southwest Montana: U.S. Geological Survey Open-File Report 82-148, 181 p.

Harlan, S.S., Snee, L.W., Reynolds, M.W., Mehnert, H.H., Schmidt, R.G., and Irving, A.J., 2005, ^{40}Ar-^{39}Ar and K-Ar geochronology and tectonic significance of the Upper Cretaceous Adel Mountain Volcanics and spatially associated Tertiary igneous rocks, northwestern Montana: U.S. Geological Survey Professional Paper 1696, 29 p.

Harlan, S.S., Geissman, J.W., Whisner, S.C., and Schmidt, C.J., 2008a, Paleomagnetism and geochronology of sills of the Doherty Mountain area, southwestern Montana: Implications for the timing of fold-and-thrust belt deformation and vertical-axis rotations along the southern margin of the Helena salient: Geological Society of America Bulletin, v. 120, no. 9–10, p. 1091–1104, https://doi.org/10.1130/B26313.1

Harlan, S.S., Geissman, J.W., and Snee, L.W., 2008b, Paleomagnetism of Proterozoic mafic dikes from the Tobacco Root Mountains, southwest Montana: Precambrian Research, v. 163, no. 3–4, p. 239–264, doi: https://doi.org/10.1016/j.precamres.2007.12.002

Harrison, J.E., Griggs, A.B., and Wells, J.D., 1986, Geologic and structure maps of the Wallace 1° x 2° quadrangle, Montana and Idaho: U.S. Geological Survey Miscellaneous Investigations Series Map I-1509-A, scale 1:250,000.

Hildebrand, R.S., 2013, Mesozoic assembly of the North American Cordillera: Geological Society of America Special Paper 495, 169 p.

Hildebrand, R.S., and Whalen, J.B., 2017, The tectonic setting and origin of Cretaceous batholiths within the North American Cordillera: The case for slab failure magmatism and its significance for crustal growth: Geological Society of America Special Paper 532, 115 p.

Houston, R.A., and Dilles, J.H., 2013, Structural geologic evolution of the Butte district, Montana: Economic Geology, v. 108, p. 1397–1424.

Hyndman, D.W., 1983, The Idaho Batholith and associated plutons, Idaho and western Montana, *in* Roddick, J.A., ed., Circum-Pacific plutonic terranes: Geological Society of America Memoir 159, p. 213–240.

Hyndman, D.W., and Alt, D., 1987, Radial dikes, laccoliths and gelatin models: Journal of Geology, v. 95, no. 6, p. 763–774.

Hyndman, D.W., Obradovich, J.D., and Ehinger, R., 1972, Potassium-argon age determinations of the Philipsburg Batholith: Geological Society of America Bulletin, v. 83, p. 473.

Hyndman, D.W., Talbot, J.L., and Chase, R.B., 1975, Boulder Batholith: A result of emplacement of a block detached from the Idaho Batholith infrastructure?: Geology, v. 3, p. 401–404.

Hyndman, D.W., Silverman, A.J., Ehinger, R., Benoit, W.R., and Wold, R., 1982, The Philipsburg Batholith: Montana Bureau of Mines and Geology Memoir 49, 37 p.

Ivy, S.D., 1988, Source, evolution, and eruptive history of the Cold Spring Creek volcanics, Beaverhead County, Montana: Corvallis, Oregon State University, M.S. thesis, 132 p.

Johnson, L.M., 1986, An overlap zone between a Laramide Rocky Mountain foreland structure and Sevier-style thrust structures near Bannack, Montana: Missoula, University of Montana, M.S. thesis, 47 p., 2 sheets, scale: 1:24,000.

Kalakay, T.J., 2001, The role of magmatism during crustal shortening in the retroarc fold and thrust belt of southwest Montana: Laramie, University of Wyoming, Ph.D. dissertation, 204 p.

Kalakay, T.J., John, B.E., and Lageson, D.R., 2001, Fault-controlled pluton emplacement in the Sevier fold-and-thrust belt of southwest Montana, USA: Journal of Structural Geology, v. 23, no. 6–7, p. 1151–1165, doi: https://doi.org/10.1016/S0191-8141(00)00182-6

King, J.T., 1997, Facies analysis of the volcaniclastic Two Medicine Formation, Wolf Creek, Montana: Missoula, University of Montana, M.S. thesis, 54 p.

Klepper, M.R., Weeks, R.A, and Ruppel, E.T., 1957, Geology of the southern Elkhorn Mountains, Jefferson and Broadwater Counties, Montana: U.S. Geological Survey Professional Paper 292, 82 p., doi: https://doi.org/10.3133/pp292

Klepper, M.R., Robinson, G.D., and Smedes, H.W., 1971a, On the nature of the Boulder Batholith of Montana: Geological Society of America Bulletin, v. 82, p. 1563–1580.

Klepper, M.R., Ruppel, E.T., Freeman, V.L., and Weeks, R.A., 1971b, Geology and mineral deposits, east flank of the Elkhorn Mountains, Broadwater County, Montana: U.S. Geological Survey Professional Paper 665, 66 p., doi: https://doi.org/10.3133/pp665

Klepper, M.R., Robinson, G.D., and Smedes, H.W., 1974, Nature of the Boulder Batholith of Montana: Discussion: Geologic Society of America Bulletin, v. 85, p. 1953–1960.

Knechtel, M.M., and Patterson, S.H., 1956, Bentonite deposits in marine Cretaceous formations, Hardin District, Montana and Wyoming: U.S. Geological Survey Bulletin 1023, 116 p., doi: https://doi.org/10.3133/b1023

Knopf, A., 1914, Is the Boulder Batholith a laccolith? (Discussion): Economic Geology, v. 9, p. 396–402.

Korzeb, S.L., Scarberry, K.C., and Zimmerman, J.L., 2018, Interpretations and genesis of Cretaceous age veins and exploration potential for the Emery mining district, Powell County, Montana: Montana Bureau of Mines and Geology Bulletin 137, 49 p.

Lageson, D., Schmitt, J., Horton, B., Kalakay, T., and Burton, B., 2001, Influence of Late Cretaceous magmatism on the Sevier orogenic wedge, western Montana: Geology, v. 29, no. 8, p. 723–726, doi: https://doi.org/10.1130/0091-7613(2001)029%3C0723:IOLCMO%3E2.0.CO;2

Lageson, D.R., Kalakay, T.J., and Foster, D.A., 2019, Emplacement of large-volume felsic plutons in active fold-thrust belts: A review of models for the Boulder Batholith (Montana) and new ideas: Northwest Geology, v. 48, p. 15–20.

Lawson, A.C., 1914, Is the Boulder "Batholith" a laccolith?—A problem in ore genesis: California University Department of Geology Bulletin, v. 8, no. 1, p. 1–15.

Lee, C.-T.A., Morton, D.M., Kistler, R.W., and Baird, A.K., 2007, Petrology and tectonics of Phanerozoic continent formation: From island arcs to accretion and continental arc magmatism: Earth and Planetary Science Letters, v. 263, p. 370–387, doi: https://doi.org/10.1016/J.EPSL.2007.09.025

Lewis, R.S., Link, P.K., Stanford, L.R., and Long, S.P., 2012, Geologic map of Idaho: Idaho Geological Survey M-9, scale 1:750,000.

Lindgren, W., 1886, Eruptive rocks of Montana: U.S. 10th Census, v. 15, p. 719–737.

Lipman, P.W., 1984, The roots of ash flow calderas in western North America: Windows into the tops of granitic batholiths: Journal of Geophysical Research, v. 89, no. B10, p. 8801–8841, doi: https://doi.org/10.1029/JB089iB10p08801

Lonn, J.D., and McDonald, C., 2004, Geologic map of the Dickie Hills 7.5′ quadrangle, southwestern Montana: Montana Bureau of Mines and Geology Open-File Report 501, scale 1:24,000.

Lowell, W.R., 1965, Geologic map of the Bannack–Grayling area, Beaverhead County, Montana: U.S. Geological Survey Miscellaneous Geologic Investigations Map I-433, scale 1:31,680, doi: https://doi.org/10.3133/i433

Lund, K., Aleinikoff, J., Kunk, M., Unruh, D., Zeihen, G., Hodges, W., du Bray, E., and O'Neill, J., 2002, SHRIMP U-Pb and $^{40}Ar/^{39}Ar$ age contrasts for relating plutonism and mineralization in the Boulder Batholith region, Montana: Economic Geology, v. 97, no. 2, p. 241–267, doi: https://doi.org/10.2113/gsecongeo.97.2.241

Lund, K., Aleinikoff, J.N., Kunk, M.J., and Unruh, D.M., 2007, SHRIMP U-Pb and $^{40}Ar/^{39}Ar$ age constraints for relating plutonism and mineralization in the Boulder Batholith region, Montana, *in* Lund, K., ed., Earth Science Studies in Support of Public Policy Development and Land Stewardship–Headwaters Province, Idaho and Montana., p. 39–46.

Lund, K., McAleer, R.J., Aleinikoff, J.N., Cosca, M.A., and Kunk, M.J., 2018, Two-event lode-ore deposition at Butte, USA: $^{40}Ar/^{39}Ar$ and U-Pb documentation of Ag-Au polymetallic lodes overprinted by younger stockwork Cu-Mo ores and penecontemporaneous Cu lodes: Ore Geology Reviews, v. 102, p. 666–700, doi: https://doi.org/10.1016/j.oregeorev.2018.05.018

Lyden, C.J., 1948, The gold placers of Montana: Montana Bureau of Mines and Geology Memoir 26, 152 p.

Lyons, J.B., 1944, Igneous rocks of the northern Big Belt Range, Montana: Geological Society of America Bulletin, v. 55, no. 4, p. 445–472, doi: https://doi.org/10.1130/GSAB-55-445

Mackie, T.L., 1986, Tectonic influences on the petrology, stratigraphy, and structures of the Upper Cretaceous Golden Spike Formation, central-western Montana: Pullman, Washington State University, M.S. thesis, 132 p.

Marvin, R.F., Zen, E., Hammarstrom, J.M., and Mehnert, H.H., 1983, Cretaceous and Paleocene potassium-argon mineral ages of the northern Pioneer Batholith and nearby igneous rocks in southwest Montana: Isochron/West, v. 38, p. 11–16.

Marvin, R.F., Zartman, R.E., Obradovich, J.D., and Harrison, J.E., 1984, Geochronometric and lead isotope data on samples from the Wallace 1° x 2° quadrangle, Montana and Idaho: U.S. Geological Survey Miscellaneous Field Studies Map MF-1354-G, scale 1:250,000.

Marvin, R.F., Mehnert, H.H., Naeser, C.W., and Zartman, R.E., 1989, U.S. Geological Survey radiometric ages—Compilation "c" part five: Colorado, Montana, Utah and Wyoming: Isochron/West, v. 53, p. 14–19.

McClelland, W.C., Tikoff, B., and Manduca, C.A., 2000, Two-phase evolution of accretionary margins: Examples from the North American Cordillera: Tectonophysics, v. 326, no. 1-2, p. 37–55, doi: https://doi.org/10.1016/S0040-1951(00)00145-1

Menold, C.A., Manning, C.E., Yin, A., Tropper, P., Chen, X.-H., and Wang, X.-F., 2009, Metamorphic evolution, mineral chemistry and thermobarometry of orthogneiss hosting ultrahigh-pressure eclogites in the North Qaidam Metamorphic Belt, western China: Journal of Asian Earth Sciences, v. 35, no. 3–4, p. 273–284, doi: https://doi.org/10.1016/j.jseaes.2008.12.008

Merrill, G.P., 1895, Notes on some eruptive rocks from Gallatin, Jefferson, and Madison Counties, Montana: U.S. National Museum Proceedings, v. 17, p. 637–673.

Miller, R.B., and Snoke, A.W., 2009, The utility of crustal cross sections in the analysis of orogenic processes in contrasting tectonic settings, *in* Miller, R.B., and Snoke, A.W., eds., Crustal cross sections from the Western North American Cordillera and elsewhere: Implications for tectonic and petrologic processes: Geological Society of America Special Paper 456, p. 1–38.

Mosolf, J., 2019, Late Cretaceous magmatism and upper crustal shortening within the Bannack volcanic field, southwest Montana, *in* Proceedings of the Montana Mining and Mineral Symposium 2018, Scarberry, K.C., and Barth, S., eds., 2018, Montana Bureau of Mines and Geology Special Publication 120, p. 63–69.

Mosolf, J., in review a, Geologic map of the Dalys 7.5' quadrangle, Beaverhead County, Montana: Montana Bureau of Mines and Geology Open-File Report, 1 sheet, 1:24,000 scale.

Mosolf, J., in review b, Geologic map of the Bannack 7.5' quadrangle, Beaverhead County, Montana: Montana Bureau of Mines and Geology Open-File Report, 1 sheet, 1:24,000 scale.

Mosolf, J.G., Kalakay, T.J., and Foster, D.A., 2020, Eocene magmatism and coeval crustal extension in Montana, *in* Metesh, J.J., and Vuke, S.M., eds., Geology of Montana—Geologic History: Montana Bureau of Mines and Geology Special Publication 122, v. 1.

Mueller, P.A., Heatherington, A.L., D'Arcy, K.A., Wooden, J.L., and Nutman, A.P., 1996, Contrasts between Sm–Nd whole-rock and U–Pb zircon systematics in the Tobacco Root Batholith, Montana: Implications for the determination of crustal age provinces: Tectonophysics, v. 265, no. 1–2, p. 169–179, doi: https://doi.org/10.1016/S0040-1951(96)00151-5

Mueller, P., Mogk, D., and Wooden, J., 2012, Age and composition of crystalline basement in the Armstead anticline, southwestern Montana: Northwest Geology, v. 41, p. 63–70.

Murphy, J.G., 2000, Geochronology of late synkinematic plutons in the Sevier fold and thrust belt, SW Montana: Gainesville, University of Florida, M.S. thesis, 105 p.

Murphy, J.G., Foster, D.A., Kalakay, T.J., John, B.E., and Hamilton, M., 2002, U-Pb zircon geochronology of the eastern Pioneer igneous complex, SW Montana: Magmatism in the foreland of the Cordilleran fold and thrust Belt: Northwest Geology, p. 1–11.

Mutch, T.A., 1960, Geology of the northeast flank of the Flint Creek Range, Montana: Princeton, New Jersey, Princeton University, Ph.D. dissertation, 159 p.

Mutch, T.A., 1961, Geology of the northeast flank of the Flint Creek Range, western Montana: Montana Bureau of Mines and Geology Geologic Map 5, scale 1:63,360.

Naibert, T.J., Geissman, J.W., and Heizler, M.T., 2010, Magnetic fabric, paleomagnetic, and $^{40}Ar/^{39}Ar$ geochronologic data bearing on the emplacement of the Late Cretaceous Philipsburg Batholith, SW Montana fold-and-thrust belt: Lithosphere, v. 2, p. 303–327, doi: https://doi.org/10.1130/L83.1

Olson, N.H., Dilles, J.H., Kallio, I.M., Horton, T.R., and Scarberry, K.C., 2016, Geologic map of the Ratio Mountain 7.5′ quadrangle, southwest Montana: Montana Bureau of Mines and Geology EDMAP-10, scale 1:24,000.

Olson, N.H., Sepp, M.D., Dilles, J.H., Mankins, N.E., Blessing, J.M., and Scarberry, K.C., 2017, Geologic map of the Mount Thompson 7.5′ quadrangle, southwest Montana: Montana Bureau of Mines and Geology EDMAP-11, scale 1:24,000.

Pearson, R.C., and Childs, J.F., 1989, Field trip guide, roadlog, and summary of Cretaceous volcanic geology, Dillon to Bannack, Beaverhead County, Montana: Northwest Geology, v. 18, p. 36–59.

Prostka, H.J., 1966, Igneous geology of the Dry Mountain quadrangle, Jefferson County, Montana: U.S. Geological Survey Bulletin 1221-F, 21 p., scale 1:24,000, doi: https://doi.org/10.3133/b1221F

Reed, M., and Dilles, J., 2020, Ore deposits of Butte, Montana, *in* Metesh, J.J., and Gammons, C.H., eds., Geology of Montana—Special Topics: Montana Bureau of Mines and Geology Special Publication 122, v. 2, 41 p.

Roberts, A.E., 1963, The Livingston Group of south-central Montana, *in* Short papers in geology and hydrology: U.S. Geological Survey Professional Paper 475-B, p. B86–B92, doi: https://doi.org/10.3133/pp475B

Roberts, A.E., 1972, Cretaceous and early Tertiary depositional and tectonic history of the Livingston area, southwestern Montana: U.S. Geological Survey Professional Paper 526-C, 119 p., doi: https://doi.org/10.3133/pp526C

Roberts, S., 1973, Pervasive early alteration in the Butte district, Montana, *in* Miller, R., ed., Guidebook for the Butte Field Meeting of the Society of Economic Geologists: Butte, Montana, The Anaconda Company, p. HH1–HH8.

Roberts, S., 1975, Early hydrothermal alteration and mineralization in the Butte district, Montana: Cambridge, Mass., Harvard University, Ph.D. dissertation, 173 p.

Roberts, E.M., and Hendrix, M.S., 2000, Taphonomy of a petrified forest in the Two Medicine Formation (Campanian), northwest Montana: Implications for palinspastic restoration of the Boulder Batholith and Elkhorn Mountains Volcanics: PALAIOS, v. 15, no. 5, p. 476–482, doi: https://doi.org/10.1669/0883-1351(2000)015%3C0476:TOAPFI%3E2.0.CO;2

Robertson, F.S., 1953, Geology and mineral deposits of the Zosell (Emery) mining district, Powell County, Montana: Montana Bureau of Mines and Geology Memoir 34, 29 p.

Robinson Roberts, L.N., and Kirschbaum, M.A., 1995, Paleogeography of the Late Cretaceous of the Western Interior of middle North America—Coal distribution and sediment accumulation: U.S. Geological Survey Professional Paper 1561, 115 p., doi: https://doi.org/10.3133/pp1561

Ruppel, E.T., 1961, Reconnaissance geologic map of the Deer Lodge quadrangle, Powell and Jefferson Counties, Montana: U.S. Geological Survey Mineral Investigations Map MF-174, scale 1:48,000.

Ruppel, E.T., 1963, Geology of the Basin quadrangle, Jefferson, Lewis and Clark, and Powell Counties, Montana: U.S. Geological Survey Bulletin 1151, 121 p., scale 1:48,000.

Ruppel, E.T., O'Neill, J.M., and Lopez, D.A., 1993, Geologic map of the Dillon 1° x 2° quadrangle, Idaho and Montana: U.S. Geological Survey Miscellaneous Investigations Series Map I-1803-H, scale 1:250,000, doi: https://doi.org/10.3133/i1803H

Rusk, B.G., Reed, M.H., and Dilles, J.H., 2008, Fluid inclusion evidence for magmatic–hydrothermal fluid evolution in the porphyry copper–molybdenum deposit at Butte, Montana: Economic Geology 103, p. 307–334, doi: https://doi.org/10.2113/GSECONGEO.103.2.307

Rutland, C., Smedes, H., Tilling, R., and Greenwood, W., 1989, Volcanism and plutonism at shallow crustal levels: The Elkhorn Mountains Volcanics and the Boulder Batholith, southwestern Montana, *in* Henshaw, P., ed., Volcanism and plutonism of western North America: Cordilleran volcanism, plutonism, and magma generation at various crustal levels, Montana and Idaho, Field trips for the 28th International Geological Congress: American Geophysical Union, Monograph, v. 2, p. 16–31.

Saleeby, J.B., Busby-Spera, C., Oldow, J.S., Dunne, G.C., Wright, J.E., Cowan, D.S., Walker, N.W., and Allmendinger, R.W., 1992, Early Mesozoic tectonic evolution of the western U.S. Cordillera, *in* Burchfiel, B.C., Lipman, P., and Zoback, M.L., eds., The Cordilleran Orogen: Conterminous U.S.: Boulder, Colo., Geological Society of America, The Geology of North America, v. G-3, p. 107–168.

Sarkar, A., Brophy, J.G., Ripley, E.M., Li, C., and Kamo, S.L., 2009, Geochemical and isotopic studies of the Lady of the Lake intrusion and associated Tobacco Root Batholith: Constraints on the genetic relation between Cretaceous mafic and silicic magmatism in southwestern Montana: Lithos, v. 113, no. 3–4, p. 555–569, doi: https://doi.org/10.1016/j.lithos.2009.06.022

Sassman, O., 1941, Metal mining in historic Beaverhead County: Bozeman, Montana State University, M.A. thesis, 310 p.

Sauer, K.B., Gordon, S.M., Miller, R.B., Vervoort, J.D., and Fisher, C.M., 2017, Evolution of the Jura-Cretaceous North American Cordilleran margin: Insights form detrital-zircon U-Pb and Hf isotopes of sedimentary units of the North Cascades Range, Washington: Geosphere, v. 13, no. 6, p. 2094–2118, doi: https://doi.org/10.1130/GES01501.1

Scarberry, K.C., 2016a, Geologic map of the Sugarloaf Mountain 7.5′ quadrangle, Deer Lodge, Jefferson, and Powell Counties, MT: Montana Bureau of Mines and Geology Open-File Report 674, scale 1:24,000.

Scarberry, K.C., 2016b, Geologic map of the Wilson Park 7.5′ quadrangle, southwestern Montana: Montana Bureau of Mines and Geology Geologic Map 66, scale 1:24,000.

Scarberry, K.C., Kallio, I.M., Olson III, N., Dilles, J.H., Older, C.W., Horton, T., and English, A.R., 2016, Large-volume pyroclastic deposits along the eastern edge of the Boulder Batholith, southwestern Montana: Geological Society of America

Abstracts with Programs, v. 48, no. 4, doi: https://doi.org/10.1130/abs/2016CD-274221

Scarberry, K.C., Kallio, I.M., and English, A.R., 2017, Geologic map of the Boulder East 7.5′ quadrangle, southwestern Montana: Montana Bureau of Mines and Geology Geologic Map 68, scale 1:24,000.

Scarberry, K.C., Coppage, E.L., and English, A.R., 2018, Geologic map of the Bison Mountain 7.5′ quadrangle, Powell and Jefferson Counties, Montana: Montana Bureau of Mines and Geology Geologic Map 71, 10 p., 1 sheet, scale 1:24,000.

Scarberry, K.C., Gammons, C.H., and Kallio, I.M., 2019a, Field guide to the geology and metallic mineral deposits along the eastern contact between the Boulder Batholith, the Elkhorn Mountains Volcanic Field, and Cretaceous-Paleozoic sedimentary rocks: Northwest Geology, v. 48, p. 61–70.

Scarberry, K.C., Coppage, E.L., and English, A.R., 2019b, Field guide to the geology and metallic mineral deposits along the western contact between the Boulder Batholith and the lower and middle members of the Elkhorn Mountains Volcanic Field: Northwest Geology, v. 48, p. 97–107.

Schmidt, C., Smedes, H., and O'Neill, M., 1990, Syncompressional emplacement of the Boulder and Tobacco Root Batholiths (Montana-USA) by pull-apart along old fault zones: Geological Journal, v. 25, no. 3–4, p. 305–318, doi: https://doi.org/10.1002/gj.3350250313

Schmidt, R.G., 1978, Rocks and mineral resources of the Wolf Creek area, Lewis and Clark, and Cascade Counties, Montana: U.S. Geological Survey Bulletin 144, 91 p., doi: https://doi.org/10.3133/b1441

Schwartz, T.M., and Schwartz, R.K., 2013, Paleogene postcompressional intermontane basin evolution along the frontal Cordilleran fold-and-thrust belt of southwestern Montana: Geological Society of America Bulletin, v. 125, no. 5–6, p. 961–984.

Schwartz, T.M., Methner, K., Mulch, A., Graham, S.A., and Chamberlain, P., 2019a, Paleogene topographic and climatic evolution of the northern Rocky Mountains from integrated sedimentary and isotopic data: Geological Society of America Bulletin, v. 131, no. 7–8, p. 1203–1223.

Schwartz, T.M., Schwartz, R.K., and Weislogel, A.L., 2019b, Orogenic recycling of detrital zircons characterizes age distributions of North American Cordilleran strata: Tectonics, v. 38, p. 4320–4334.

Sears, J.W., 2016, Belt–Purcell Basin: Template for the Cordilleran magmatic arc and its detached carapace, Idaho and Montana, *in* MacLean, J.S., and Sears, J.W., eds., Belt Basin: Window to Mesoproterozoic Earth: Geological Society of America Special Paper 522, p. 365–384.

Sears, J.W., McDonald, C., and Lonn, J., 2010, Lewis and Clark Line, Montana: Tectonic evolution of a crustal-scale flower structure in the Rocky Mountains, *in* Morgan, L.A., and Quane, S.L., eds., Through the generations: Geologic and anthropogenic field excursions in the Rocky Mountains from modern to ancient: Geological Society of America Field Guide 18, p. 1–20.

Shenon, P.J., 1931, Geology and ore deposits of Bannack and Argenta, Beaverhead County, Montana: Montana Bureau of Mines and Geology Bulletin 6, 80 p.

Skipp, B., and McGrew, L.W., 1977, The Maudlow and Sedan Formations of the Upper Cretaceous Livingston Group on the west edge of the Crazy Mountains Basin, Montana: U.S. Geological Survey Bulletin 1422-B, 68 p., doi: https://doi.org/10.3133/b1422B

Skipp, B., and Peterson, A.D., 1965, Geologic map of the Maudlow quadrangle, southwestern Montana: U.S. Geological Survey Miscellaneous Geologic Investigations Map I-452, scale 1:24,000, doi: https://doi.org/10.3133/i452

Skipp, B., Lageson, D.R., and McMannis, W.J., 1999, Geologic map of the Sedan quadrangle, Gallatin and Park Counties, Montana: U.S. Geological Survey Geologic Investigation Map I-2634, version 2.0, scale 1:48,000.

Smedes, H.W., 1966, Geology and igneous petrology of the northern Elkhorn Mountains, Jefferson and Broadwater Counties, Montana: U.S. Geological Survey Professional Paper 510, 116 p., doi: https://doi.org/10.3133/pp510

Smedes, H.W., 1973, Regional geologic setting of the Boulder Batholith, Montana, *in* Miller, R., ed., Guidebook for the Butte Field Meeting of the Society of Economic Geologists: Butte, Montana, The Anaconda Company, p. A-1–A-6.

Smith, R.L., 1960, Ash flows: Geological Society of America Bulletin, v. 71, no. 6, p. 795–842, doi: https://doi.org/10.1130/0016-7606(1960)71[795:AF]2.0.CO;2

Snee, L.W., 1978, Petrography, K-Ar ages, and field relations of the igneous rocks of part of the Pioneer Batholith, southwestern Montana: Columbus, Ohio State University, M.S. thesis, 110 p.

Snee, L.W., 1982, Emplacement and cooling of the Pioneer Batholith, southwestern Montana: Columbus, Ohio State University, Ph.D. dissertation, 339 p.

Spivey, R.C., 1940, Bentonite in southwestern South Dakota: South Dakota Geological Survey Report of Investigations 36, 56 p.

Tabata, H., Yamauchi, K., Maruyama, S., and Liou, J.G., 1998, Tracing the extent of a UHP metamorphic terrane: Mineral-inclusion study of zircons in gneisses from the Dabie Shan, *in* Hacker, B.R., and Liou, J.G., eds., When continents collide: Geodynamics and geochemistry of ultrahigh-pressure rocks: Netherlands, Kluwer Academic Publishing, p. 261–273.

Tatum, S.C., 2015, A gravity investigation of the Tobacco Root Batholith, southwest Montana: Kalamazoo, Western Michigan University, M.S. thesis, 67 p.

Thomas, G.M., 1981, Structural geology of the Badger Pass area, southwest Montana: Missoula, University of Montana, M.S. thesis, 58 p., 1 sheet, scale: 1:24,000.

Thomas, R.G., Eberth, D.A., Deino, A.L., and Robinson, D., 1990, Composition, radioisotopic ages, and potential significance of an altered volcanic ash (bentonite) from the Upper Cretaceous Judith River Formation, Dinosaur Provincial Park, southern Alberta, Canada: Cretaceous Research, v. 11, no. 2, p. 125–162, doi: https://doi.org/10.1016/S0195-6671(05)80030-8

Tikoff, B., Kelso, P., Manduca, C., Markley, M.J., and Gillaspy, J., 2001, Lithospheric and crustal reactivation of an ancient plate boundary: The assembly and disassembly of the Salmon River suture zone, Idaho, USA, *in* Holdsworth, R.E., and others, eds., Fault reactivation: Geologic Society of London Special Publication 186, p. 213–231.

Tilling, R.I., 1973, Boulder Batholith, Montana—A product of two contemporaneous but chemically distinct magma series: Geological Society of America Bulletin, v. 84, no. 12, p. 3879–3900, doi: https://doi.org/10.1130/0016-7606(1973)84%3C3879:BBMAPO%3E2.0.CO;2

Tilling, R.I., 2000, Mount St. Helens 20 years later: What we've learned: Geotimes, v. 45, p. 14–19.

Tilling, R.I., Klepper, M.R., and Obradovich, J.D., 1968, K-Ar ages and time span of emplacement of the Boulder Batholith, Montana: American Journal of Science, v. 266, p. 671–689.

Tipper, H.W., Woodsworth, G.J., and Gabrielse, H., 1981, Tectonic assemblage map of the Canadian Cordillera and adjacent parts of the United States of America: Geological Survey of Canada Map 1505A, scale 1:2,000,000.

Tysdal, 2000, Revision of middle Proterozoic Yellowjacket Formation, central Idaho, and revision of Cretaceous Slim Sam Formation, Elkhorn Mountains area, Montana: U.S. Geological Survey Professional Paper 1601-B, 21 p., doi: https://doi.org/10.3133/pp1601AB

Vejmelek, L., and Smithson, S., 1995, Seismic reflection profiling in the Boulder Batholith, Montana: Geology, v. 23, no. 9, p. 811–814, doi: https://doi.org/10.1130/0091-7613(1995)023%3C0811:SRPITB%3E2.3.CO;2

Viele, G.W., and Harris, F.G., III, 1965, Montana Group stratigraphy, Lewis and Clark County, Montana: American Association of Petroleum Geologists Bulletin, v. 49, no. 4, p. 379–417, doi: https://doi.org/10.1306/A663362C-16C0-11D7-8645000102C1865D

Vuke, S.M., Porter, K.W., Lonn, J.D., and Lopez, D.A., 2007, Geologic map of Montana: Montana Bureau of Mines and Geology Geologic Map 62A, scale 1:500,000.

Waddell, A.M., 1997, Cordilleran partitioning and foreland basin evolution as recorded by the sedimentation and stratigraphy of the Upper Cretaceous Carter Creek and Golden Spike Formations, central-western Montana: Missoula, University of Montana, M.S. thesis, 148 p.

Walker, S.C., 1987, The nature and origin of bentonites and potassium bentonites, northwestern Montana: Missoula, University of Montana, M.S.

thesis, 33 p.

Weed, W.H., 1893, The Laramie and the overlying Livingston Formation in Montana: U.S. Geological Survey Bulletin 105, 68 p.

Weed, W.H., 1901, Geology and ore deposits of the Elkhorn mining district, Jefferson County, Montana: U.S. Geological Survey 22nd Annual Report, Part 2, p. 407–510.

Weeks, R.A., 1974, Geologic map of the Bull Mountain area, Jefferson County, Montana: U.S. Geological Survey Open-File Report 74-354, scale 1:48,000, doi: https://doi.org/10.3133/ofr74354

Woodward, L.A., 1986, Tectonic origin of fractures for fissure vein emplacement in the Boulder Batholith and adjacent rocks, Montana: Economic Geology, v. 81, no. 6, p. 1387–1395, doi: https://doi.org/10.2113/gsecongeo.81.6.1387

Ye, K., Cong, B., and Ye, D., 2000, The possible subduction of continental material to depths greater than 200 km: Nature, v. 407, p. 734–736.

Yonkee, W.A., and Weil, A.B., 2015, Tectonic evolution of the Sevier and Laramide belts within the North American Cordillera orogenic system: Earth Science Reviews, v. 150, p. 531–593, doi: https://doi.org/10.1016/j.earscirev.2015.08.001

Zen, E., 1996, Plutons in the eastern part of the Pioneer Batholith: Field relations and petrographic descriptions: U.S. Geological Survey Open-File Report 96–97, 98 p.

Zen, E., Marvin, R.F., and Mehnert, H.H., 1975, Preliminary petrographic, chemical, and age data on some intrusive and associated contact metamorphic rocks, Pioneer Mountains, southwestern Montana: Geological Society of America Bulletin, v. 86, no. 3, p. 367–370, doi: https://doi.org/10.1130/0016-7606(1975)86%3C367:PPCAAD%3E2.0.CO;2